Journal of Dermatological Science 69 (2013) 250–258

Contents lists available at SciVerse ScienceDirect

Journal of Dermatological Science

journal homepage: www.elsevier.com/jds

Chemokine receptors CCR2 and CX3CR1 regulate skin fibrosis in the mouse model of cytokine-induced systemic sclerosis☆

Minako Arai [a], Yuka Ikawa [a], Sonoko Chujo [a], Yasuhito Hamaguchi [a], Wataru Ishida [a], Fumiaki Shirasaki [a], Minoru Hasegawa [a], Naofumi Mukaida [b], Manabu Fujimoto [a], Kazuhiko Takehara [a,*]

[a] Department of Dermatology, Kanazawa University Graduate School of Medical Science, Ishikawa, Japan
[b] Department of Molecular Oncology, Cancer Research Institute, Kanazawa University, Japan

ARTICLE INFO

Article history:
Received 11 June 2012
Received in revised form 2 October 2012
Accepted 17 October 2012

Keywords:
Systemic sclerosis
Transforming growth factor-β
Connective tissue growth factor
Macrophage chemoattractant protein-1
Fractalkine

ABSTRACT

Background: Skin fibrotic disorders such as systemic sclerosis (SSc) are characterized by an excessive accumulation of extracellular matrix (ECM), and develop under the influence of certain cytokines. We previously established a mouse model of skin fibrosis induced by exogenous application of cytokines. We have revealed that both the number of macrophages and the levels of macrophage chemoattractant protein-1 (MCP-1) mRNA positively correlate with the extent of skin fibrosis. Macrophages can be divided into two subsets, the first expressing CCR2, and the second expressing CX3CR1.
Objective: To elucidate the role of skin infiltrating macrophages based on CCR2 and CX3CR1 in this cytokine-induced murine fibrosis model.
Methods: We examined the amounts of collagen deposited in granulation tissues, the numbers of macrophages and the levels of several mRNA in wild type (WT) mice, $CCR2^{-/-}$ mice, and $CX3CR1^{-/-}$ mice during injections of transforming growth factor-β (TGF-β) followed by injections of connective tissue growth factor (CTGF).
Results: TGF-β injection increased the expressions of MCP-1, fractalkine, CCR2 and CX3CR1 mRNA in WT mice. The overproduction of collagen induced by TGF-β was significantly reduced by CCR2 deficiency, while collagen contents induced by CTGF were restored to wild-type levels. In contrast, overproduction of collagen in CX3CR1-deficient mice decreased nearly 50% by both TGF-β and CTGF stimulations.
Conclusion: The involvement of CCR2/MCP-1 interaction (CCR2-dependent loop) was during the TGF-β phase. In contrast, the fractalkine/CX3CR1 interaction contributes to the initiation of fibrosis by TGF-β and its maintenance by CTGF. Collectively, two subsets of macrophages both cooperatively and independently play important roles in the development of fibrosis.

1. Introduction

SSc is an autoimmune rheumatic disease characterized by fibrosis and vascular injury in the skin and multiple internal organs. The etiology and pathogenesis of SSc remain unclear. Clinically, SSc is typified by excessive collagen deposition, vascular damage, and immunological activation and these clinical features are likely interrelated [1–4]. The central event in the pathogenesis of SSc is an abnormal accumulation of extracellular matrix (ECM) components, predominantly type I and III collagen. The mechanisms that cause excessive fibrosis in SSc remain incompletely understood, however, many studies have suggested that cytokine release from inflammatory cells, endothelial cells, fibroblasts, and other cell types in the involved organs play important roles in the initiation and maintenance of fibrosis [5,6].

Among these cytokines, transforming growth factor-β (TGF-β) and connective tissue growth factor (CTGF) are thought to play central roles in the pathogenesis of SSc [7,8]. To understand the mechanisms of fibrosis and the contributions of cytokines better, we established a unique animal model of skin fibrosis by exogenously administering cytokines [9]. In this model, the in vivo effects of cytokines are examined following subcutaneous injection into newborn mice. We found previously that TGF-β induced only transient fibrosis on day 4, despite 7 days of consecutive injections [10]. By contrast, serial injections of CTGF after TGF-β administration caused persistent fibrosis [11]. We also identified a positive correlation between the number of macrophages present, MCP-1 mRNA expression levels, and the extent of skin fibrosis [12]. This finding suggested that macrophages and

☆ This work was supported by a Grant-in-Aid from the Ministry of Education, Science, and Culture of Japan.
* Corresponding author at: Department of Dermatology, Kanazawa University Graduate School of Medical Science, 13-1 Takara-machi, Kanazawa, Ishikawa 920-8641, Japan. Tel.: +81 76 265 2343; fax: +81 76 234 4270.
E-mail address: takehara@med.kanazawa-u.ac.jp (K. Takehara).

0923-1811/$36.00
http://dx.doi.org/10.1016/j.jdermsci.2012.10.010

macrophage related cytokines might indirectly contribute to the development of fibrosis.

Activated macrophages appear to play an important role in fibrosis because they are among the first immune cells recruited during the initial stages of fibrosis. It has long been known that early SSc skin contains an increased number of CD14-positive cells (monocytes/macrophages), compared to normal skin [13]. When activated, macrophages release a number of pro-inflammatory and fibrogenic mediators, such as TGF-β and platelet-derived growth factor (PDGF) [14]. Macrophages are classified into two functional subsets based on their chemokine receptor expression pattern: a short-lived CCR2 subset that is actively recruited to inflamed tissues, and a CX3CR1 subset characterized as resident in non-inflamed tissues [15]. CCR2 is a major receptor for MCP-1, while CX3CR1 is a receptor for fractalkine, a chemokine expressed by endothelial cells.

MCP-1 stimulates collagen production by fibroblasts via endogenous upregulation of TGF-β expression [16]. Previous studies have demonstrated that MCP-1 gene expression is increased during bleomycin-induced pulmonary fibrosis in mice [17] and interstitial kidney fibrosis [18]. In SSc patients, serum levels of MCP-1 are elevated, and spontaneous MCP-1 production by peripheral blood mononuclear cells is increased relative to normal controls [19]. MCP-1 is also strongly expressed in the epidermis, in inflammatory mononuclear cells, and in endothelial cells in the sclerotic skin of SSc patients, but it is not expressed in normal skin. Administration of anti-MCP-1 neutralizing antibody reduced skin sclerosis in bleomycin-treated mice [20]. Furthermore, mice deficient for the MCP-1 receptor CCR2 are protected from fluoresceinisothiocyanate-induced and bleomycin-induced lung fibrosis [21,22]. Thus, it appears that MCP-1 is critically involved in the pathogenesis of SSc.

Fractalkine is a membrane-bound chemokine that functions not only as a chemoattractant but also as an adhesion molecule, and it is expressed on proinflammatory cytokine activated endothelial cells. The fractalkine receptor, CX3CR1, is expressed on mature monocytes, NK cells, and cytotoxic effector T cells [23]. We previously demonstrated that fractalkine was strongly expressed on endothelial cells in affected skin and lung tissues in SSc patients. Additionally, soluble fractalkine levels were significantly elevated in sera and were associated with the existence of digital ischemia, and severe pulmonary fibrosis. The number of CX3CR1-expressing cells, including monocytes, was increased in the lesional skin and lung tissues from SSc patients with diffuse cutaneous involvement [24]. Collectively, these data suggest a role for fractalkine as a major mediator of SSc.

In this study, we have investigated whether CCR2/MCP-1 or CX3CR1/fractalkine play a role in the induction and maintenance of skin fibrosis in our animal model, to determine if these molecules might be useful as novel therapeutic targets in fibrotic disorders.

2. Materials and methods

2.1. Mice

Specific pathogen-free 8–10-week-old female BALB/c mice (WT mice) were purchased from Charles River Japan (Yokohama, Japan). CCR2-deficient ($CCR2^{-/-}$) mice and CX3CR1-deficient ($CX3CR1^{-/-}$) mice were generated [25,26] and backcrossed to a BALB/c background for more than 8 generations in our animal facility. All studies and procedures were approved by the Committee on Animal Experimentation of Kanazawa University Graduate School of Medical Science.

2.2. Growth factors

Human recombinant TGF-β3 was purchased from R&D Systems, Inc. (Minneapolis, MN). Human recombinant CTGF was a generous gift from Nosan Corporation (Yokohama, Japan). Endotoxin levels of TGF and CTGF were <1.0 EU per 1 μg of cytokine as determined by the LAL method, respectively.

2.3. In vivo experimental model

TGF-β3 and CTGF were dissolved in phosphate-buffered saline (PBS), to obtain final concentrations of 40 and 20 ng/μl, respectively. Newborn mice were injected with 20 μl of TGF-β3 (800 ng), CTGF (400 ng), or with PBS as a control, into the subcutaneous neck tissue once a day for 3 or 7 consecutive days. Serial injections of the two growth factors (TGF-β3 for days 1–3 days and CTGF for days 4–7) were also conducted (Fig. 1). The amounts of growth factors used in these experiments were previously shown to be optimal in our skin fibrotic animal models using BALB/C mice [10,11]. The mice were euthanized with an overdose of diethyl ether 24 h after the final injection, and tissue samples were obtained from the site of injection. Parts of the tissue samples were fixed in 10% neutral buffered formalin and processed for routine histological examination and the measurement of collagen content. The remaining tissue was embedded in Tissue-Tek OCT compound (Miles, IN), snap frozen in liquid nitrogen, and stored at −70 °C prior to use. Ten serial 6-μm sections were cut from each frozen sample embedded in OCT compound. The sections were subjected to RNA extraction.

2.4. Measurement of collagen content in tissue samples

Tissue samples were embedded in paraffin and sections, approximately 15 μm thick, were obtained. Groups of 10–20 sections were deparaffinized after incubation with xylol, xylol:ethanol (1:1), ethanol, water:ethanol (1:1), and water. We used only granulated areas of the sections. Individual samples were placed in small test tubes and covered with 0.2 ml of a saturated solution of picric acid in distilled water that contained 0.1% Fast green FCF and 0.1% Sirius red F3BA. The samples were rinsed several times with distilled water until the fluid was colorless. One milliliter of 0.1 N NaOH in absolute methanol (1:1; v/v) was added and the eluted color was read in a spectrophotometer at 540 nm and 605 nm. The method is based on the selective binding of Sirius red F3BA and Fast green FCF to collagens and non-collagenous proteins, respectively [27]. Each experimental sample was run in triplicate.

2.5. RNA isolation and cDNA synthesis

Total RNA was extracted from frozen granulation tissue samples using RNeasy (Qiagen, Valencia, CA) spin columns, according to the manufacturer's protocol, with the addition of a DNase digestion step. RNA concentration and purity was determined spectrophotometrically by measuring fluorescence at 260 nM and 280 nM. Total RNA

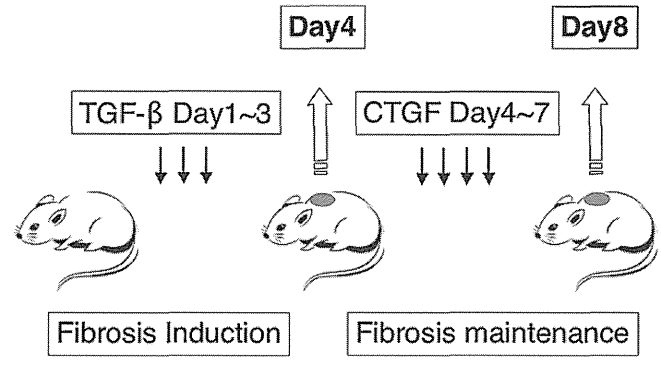

Fig. 1. Cytokine-induced fibrosis model. Serial injections of the two growth factors (TGF-β3 for days 1–3 and CTGF for days 4–7) were conducted.

(100 μg) was reverse transcribed into cDNA in a total volume of 20 μg using a Reverse Transcription System (Promega, Madison, WI) according to the manufacturer's instructions.

2.6. Taqman quantitative real-time PCR analysis

Four microliters of cDNA were used as a template for real-time PCR, which was carried out in an ABI Prism 7000 Sequence Detector System (PE Applied Biosystems, Foster city, CA). The sequences of the mouse α 2 chain of the type I collagen (*COL1A2*) primers and probe used are 5′-CAC CCC AGC GAA GAA CTC ATA-3′ (forward), 5′-GCC ACC ATT GAT AGT CTC TCC TAA C-3′ (reverse) and 5′-CGC CCA GGC CAA CAA GCA TGT C-3′ (probe). Intron-spanning primers were used to minimize the possibility of co-amplifying genomic DNA. The primers for MCP-1, fractalkine, CCR2, CX3CR1 and CTGF were purchased from Applied Biosystems. We used the Taqman rodent GAPDH control reagent (PE Applied Biosystems) as an internal control. PCR (1× (50 °C, 2 min, 95 °C, 10 min), 40× (95 °C, 15 s, 60 °C, 1 min) was performed in the presence of 0.6× Taqman Universal PCR master mix (PE Applied Biosystems), forward and reverse primers and a sequence-specific fluorescent probe. Optimal probe and primer concentrations were determined for each assay to ensure maximum specificity. Relative units (RU) were calculated by the comparative C_T method. First, the C_T for the target amplification (FAM) and the C_T for the endogenous control (VIC; GAPDH) were determined for each sample. The difference between the C_T for the target and the C_T for the internal control, called ΔC_T, was calculated to normalize for the differences in the amounts of total nucleic acid added to each mixture. The ΔC_T of the calibrator was subtracted from the ΔC_T of each experimental sample to give $\Delta\Delta C_T$. The amount of target normalized to an endogenous control and relative to the calibrator, was then calculated using the equation $2^{(-\Delta\Delta C_T)}$. Each experimental sample was run in triplicate.

2.7. Histological examination and immunohistochemistry

The formalin-fixed and paraffin-embedded specimens were cut to a thickness of 4 mm and stained with hematoxylin and eosin. Immunohistochemical analysis using antimouse F4/80 antibody (clone A3-1, ACM, UK), CD11b (clone M1/70, BD Biosciences, San Jose, CA), Gr1 (clone RB6-8C5, BD Biosciences) at a dilution 1:100 was performed with biotinylated anti-mouse IgG as secondary antibody. Visualization was done with the standard streptavidin–biotin-coupled immunoperoxidase technique (Histofine kit, Nichirei, Tokyo, Japan). The measurement of macrophages was performed by averaging the number of cells identified by positive for the F4/80 or CD11b staining per visual field in five high power fields (magnification, ×200), respectively. Each experimental sample was run in triplicate.

2.8. Macrophage isolation

Magnetic cell sorting technology (Miltenyi Biotec, Bergisch Gladbach, Germany) was used to purify macrophages according to the manufacture's instructions. CD11b microbeads were used to purify macrophages from spleen cells.

2.9. Cell culture in vitro

Primary fibroblast cultures were established from dorsal skin of newborn wild-type mice as described. Fibroblasts were grown at 37 °C in a 5% CO_2 atmosphere in Dulbecco's modified Eagle's medium (DMEM) (Wako Pure Chemical Industries, Osaka, Japan) with 10% fetal calf serum (Nunc, Roskilde, Denmark), 100 U/ml penicillin/streptomycin in 6-well multi-dishes. Passages 3–5 were used for the experiments. After cells reached confluence, the culture medium was discarded and cells were starved using DMEM with 0.1% bovine serum albumin and nonessential amino acids (Sigma, St. Louis, MO) for 24 h prior to initiating TGF-β3 or CTGF stimulation. TGF-β3 or CTGF was added to the cell culture medium to a final concentration of 10 ng/mL, 150 ng/mL after 24 h starvation. The cells were then cultured for 24 h. For macrophage-fibroblast cocultues, macrophages (5×10^5 cells per well) were added in the upper wells (insert) of a 6-well transwell plate (0.4 mm pore size; BD Falcon) simultaneously with TGF-β3. At the end of each experiment, total RNA was isolated from fibroblasts in the lower chamber using RNeasy (Qiagen, Valencia, CA) as above. To examine a contamination by endothelial cells, we added the FACS analyses of skin fibroblasts. CD31+ cells were not detected in isolated skin fibroblasts by FACS analysis (data not shown).

2.10. Flow cytometry

Abs used in this study included PE-conjugated anti-CCR2 mAb (R&D Systems, Minneapolis, MN), APC-conjugated anti-CX3CR1 mAb(R&D Systems). Single-cell suspensions of isolated macrophages were incubated with the Abs for 30 min at 4 °C. The cells washed and fixed with 1% paraformaldehyde in PBS. Stained Samples were analyzed on FACSVantage SE (BD Biosciences), analyzing data from 10^5 cells. Data were analyzed using the FlowJo (Tree Star, Ashland, OR) software. Positive and negative populations of cells were determined using unreactive isotype-matched mAbs (BD Biosciences) as controls for background staining.

2.11. Statistical analysis

Values were expressed as the mean ± SEM. Student's *t*-test was used to evaluate the statistical differences between the groups.

3. Results

3.1. Semi-quantitative analysis of collagen content in skin fibrosis induced by exogenous injection of TGF-β and CTGF in CCR2-KO and CX3CR1-KO mice

We previously showed that serial injections of CTGF after TGF-β induced persistent fibrotic tissue formation in newborn mice [11], leading to increased amounts of deposited collagen in granulation tissue [12]. We next wanted to analyze the requirements for the chemokine receptors CCR2 and CX3CR1 in this same model system in order to examine potential roles for chemokines in SSc. In this study, we injected 800 ng of TGF-β on days 1–3 followed by 400 ng of CTGF on days 4–7. Since the profibrogenic effects of TGF-β1, -β2, and -β3 were almost identical in previous experiments [10], we used TGF-β3 (henceforth referred to as TGF-β) for all experiments in the present study.

Serial injections of CTGF following TGF-β administration caused a prominent collagen accumulation in WT mice (Fig. 2A and E). By contrast, the collagen content was not increased in $CCR2^{-/-}$ mice until day 4, resulting in a significant reduction of local collagen as compared with WT mice ($p < 0.005$) (Fig. 2A and C). However, during days 5–8, when CTGF was injected, enhanced collagen production was observed in $CCR2^{-/-}$ mice, resulting in equivalent collagen content levels in $CCR2^{-/-}$ mice and WT mice at day 8 (Fig. 2A and F). In $CX3CR1^{-/-}$ mice, collagen levels were decreased by approximately 50% on days 4 and 8 as compared with WT mice ($p < 0.05$ and $p < 0.005$, respectively) (Fig. 2A, D and G). These semi-quantitative results were for the most part consistent with the histological findings. The collagen contents injected with

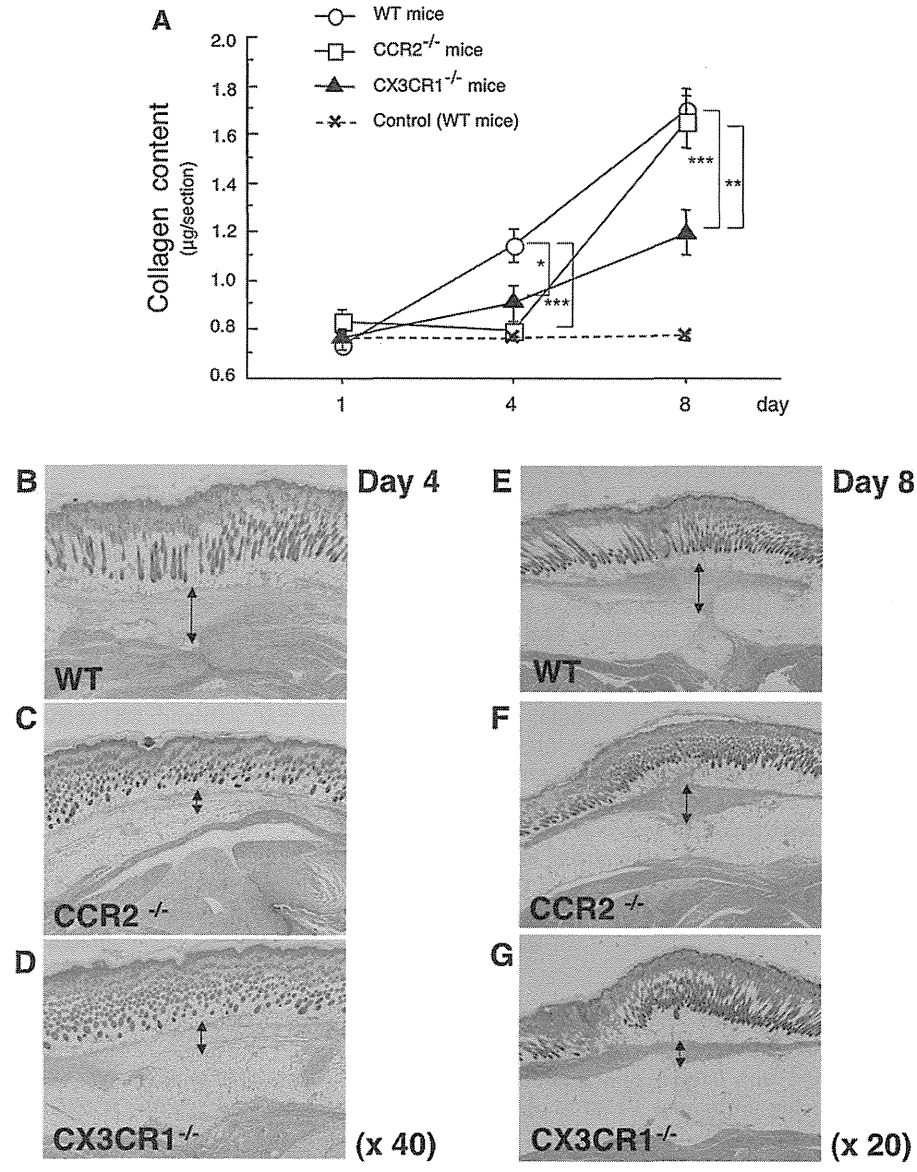

Fig. 2. (A) The amounts of collagen deposited in granulation tissues in WT mice, CCR2$^{-/-}$ mice, and CX3CR1$^{-/-}$ mice during injections of 800 ng of TGF-β on days 1–3 followed by injections of 400 ng of CTGF on days 4–7. Control WT mice were treated with PBS. Values are the mean ± SEM of 4–7 mice in each group. $^{*}p < 0.05$, $^{**}p < 0.01$, $^{***}p < 0.005$. (B)–(G) Representative histopathology from WT mice (B), CCR2$^{-/-}$ mice (C), and CX3CR1$^{-/-}$ mice (D) on day 4, and WT mice (E), CCR2$^{-/-}$ mice (F), and CX3CR1$^{-/-}$ mice (G) on day 8.

PBS as control were not increased in WT, CCR2$^{-/-}$, or CX3CR1$^{-/-}$ mice (data not shown).

3.2. mRNA levels for the α2 chain of type 1 collagen in granulation tissues

We next investigated mRNA levels for the α2 chain of type I collagen (COL1A2) in granulation tissues. The levels of COL1A2 were determined by real-time PCR and normalized against the GAPDH mRNA level in each sample. As shown in Fig. 3, just TGF-β induced a significant increase in the amount of COL1A2 mRNA in WT mice on day 4 ($p < 0.05$). The level of COL1A2 mRNA at day 4 was reduced in CCR2$^{-/-}$ and CX3CR1$^{-/-}$ mice, but were still greater than that observed in WT mice in the absence of TGF-β. These data suggest that the increased collagen content observed after TGF-β administration is due to alterations at the transcriptional level. As shown in Fig. 4, CTGF following TGF-β induced an increase in the amount of COL1A2 mRNA in WT mice on day 8.

3.3. Profile of inflammatory cells in this animal model of skin fibrosis

It has been reported that the numbers of macrophages are increased in fibrotic tissues [28]. In our model, TGF-β injection increased the number of lesional macrophages on day 4, and these numbers continued to increase with subsequent CTGF injections on days 4–7 [12]. The numbers of accumulated F4/80-positive cells on day 4 and 8 were significantly decreased in CCR2$^{-/-}$ mice, as compared to WT mice ($p < 0.05$ and $p < 0.001$) (Fig. 5A and C). CX3CR1$^{-/-}$ mice also exhibited an approximately 30% reduction in macrophage infiltration on day 8 ($p < 0.005$, as compared to WT mice) (Fig. 5A and D). The numbers of accumulated CD11b-positive cells on day 4 and 8 were significantly decreased in CCR2$^{-/-}$ mice, as compared to WT mice ($p < 0.05$ and $p < 0.05$) (Fig. 5E). CX3CR1$^{-/-}$ mice also exhibited a reduction in macrophage infiltration on day 8 ($p < 0.05$, as compared to WT mice) (Fig. 5E). The numbers of accumulated Gr1-positive cells on day 4 and 8 were not decreased in CCR2$^{-/-}$ and CX3CR1$^{-/-}$ mice, as

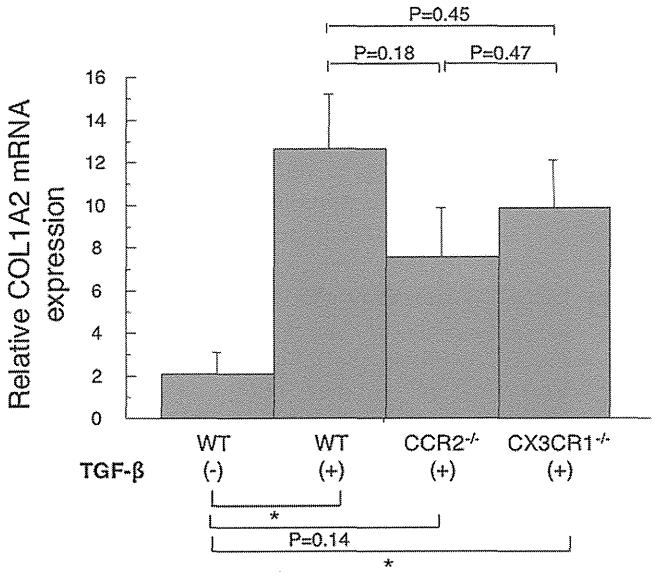

Fig. 3. mRNA levels for the α2 chain of type I collagen in granulation tissues from WT mice, $CCR2^{-/-}$ mice, and $CXCR3^{-/-}$ mice on day 4 after TGF-β injections. The expression levels of COL1A2 mRNA were determined by real-time PCR and normalized against the GAPDH mRNA expression level in each sample. Values are the mean of 4–6 mice in each group. $^{*}p < 0.05$.

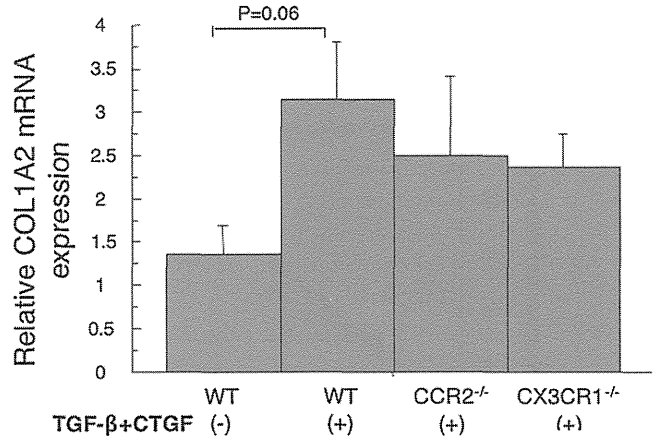

Fig. 4. mRNA levels for the α2 chain of type I collagen in granulation tissues from WT mice, $CCR2^{-/-}$ mice, and $CXCR3^{-/-}$ mice on day 8 after CTGF following TGF-β injections. The expression levels of COL1A2 mRNA were determined by real-time PCR and normalized against the GAPDH mRNA expression level in each sample. Values are the mean of 4–6 mice in each group. $^{*}p < 0.05$.

compared to WT mice (Fig. 5F). The numbers of macrophages were not increased in WT, $CCR2^{-/-}$, or $CX3CR1^{-/-}$ mice injected with PBS as control (data not shown).

3.4. Chemokine and chemokine receptor mRNA levels in granulation tissues

To examine whether chemokines produced by macrophages and inflammatory cells play a role in skin fibrosis, we performed real-time PCR analysis. TGF-β injection increased the expressions of MCP-1, fractalkine, CCR2 and CX3CR1 mRNA on day 4 in WT mice (Fig. 6). Similarly, we examined the expression of these molecules in $CCR2^{-/-}$ mice and $CX3CR1^{-/-}$ mice. As expected, CCR2 and CX3CR1 mRNA were undetectable in their respective knock-out mice. In $CX3CR1^{-/-}$ mice and $CCR2^{-/-}$ mice, each chemokine level was low, as compared to treated WT controls. In $CX3CR1^{-/-}$ mice and $CCR2^{-/-}$ mice, each chemokine receptor level was low, as compared to treated WT controls. CTGF following TGF-β injection increased the expressions of MCP-1 and fractalkine on day 8 in WT mice (Fig. 7).

3.5. Expression of CCR2 and CX3CR1 on WT macrophages

Flowcytometric analysis showed that WT $CD11b^{+}$ gated cells expressed CCR2 and CX3CR1 protein (Fig. 8).

3.6. Chemokine and chemokine receptor mRNA levels in fibroblast cultures

In macrophage-fibroblast cocultures, cultured fibroblasts possessed increased levels of not only MCP-1 mRNA, but also CTGF mRNA ($p < 0.0005$ and $p < 0.05$), compared with fibroblasts cultured alone. Stimulation with TGF-β significantly augmented fractalkine and CTGF mRNA expression in cultured fibroblasts ($p < 0.0005$ and $p < 0.0005$), and tended to augment COL1A2 mRNA. Fibroblast stimulation with CTGF augmented CTGF mRNA levels ($p < 0.05$), providing evidence for an autocrine feedback loop. In contrast, CTGF stimulation of fibroblasts did not alter fractalkine mRNA levels (Fig. 9).

4. Discussion

In the current study using a cutaneous fibrosis model, in which fibrosis is induced by serial TGF-β and CTGF injections, we have shown that macrophage-related chemokines play important roles in the development of this condition. This is consistent with our previous finding of increased number of macrophages at the CTGF injection site following TGF-β administration [12]. The current study suggests that interactions between fibroblasts and immune cells, including macrophages, contribute to the induction and maintenance of fibrosis via increased production of cytokines and chemokines.

MCP-1 is produced by macrophages, fibroblasts, endothelial cells, and other cells. MCP-1 is the predominant chemoattractant and activator of $CCR2^{+}$ monocytes and T cells. In addition to its chemoattractant activities, this chemokine induces Th2 cell polarization [29]. MCP-1 directly stimulates collagen production by fibroblasts via specific receptors and endogenous upregulation of TGF-β expression [16]. Our in vivo data also revealed that serial injections of TGF-β increased MCP-1 mRNA and CCR2 mRNA levels. Conversely, the loss of CCR2 attenuated macrophage infiltration as well as skin fibrosis at day 4. Also, in macrophage-fibroblast in vitro cocultures, fibroblasts displayed increased levels of both MCP-1 and CTGF mRNAs. The upregulated collagen levels induced by TGF-β were significantly reduced by CCR2 deficiency, while collagen levels induced by CTGF were unaffected. Thus, MCP-1 is required for TGF-β-mediated fibrosis induction in our mouse model. Collectively, the involvement of MCP-1/CCR2 interaction (CCR2-dependent loop) may be involved in the pathogenesis of skin fibrosis in which TGF-β plays a role.

Our data and previous studies estimate the following hypothesis regarding the role of MCP-1/CCR2 in the development of tissue fibrosis in SSc: first, MCP-1 augments the recruitment of CCR2-expressing macrophages and T cells into tissues, and promotes the interaction of $CCR2^{+}$ macrophages and fibroblasts. Then, TGF-β and PDGF produced by activated CCR2-expressing macrophages stimulate collagen synthesis by fibroblasts. At the same time, MCP-1 preferentially induces T cell differentiation to Th2 cells rather than Th1 cells, and IL-4-secreting Th2 cells migrate to the fibroblasts. In turn, activated fibroblasts produce MCP-1, leading to the amplification loop for the development of tissue fibrosis.

Fractalkine is a membrane-bound chemokine that functions not only as a chemoattractant but also as an adhesion molecule.

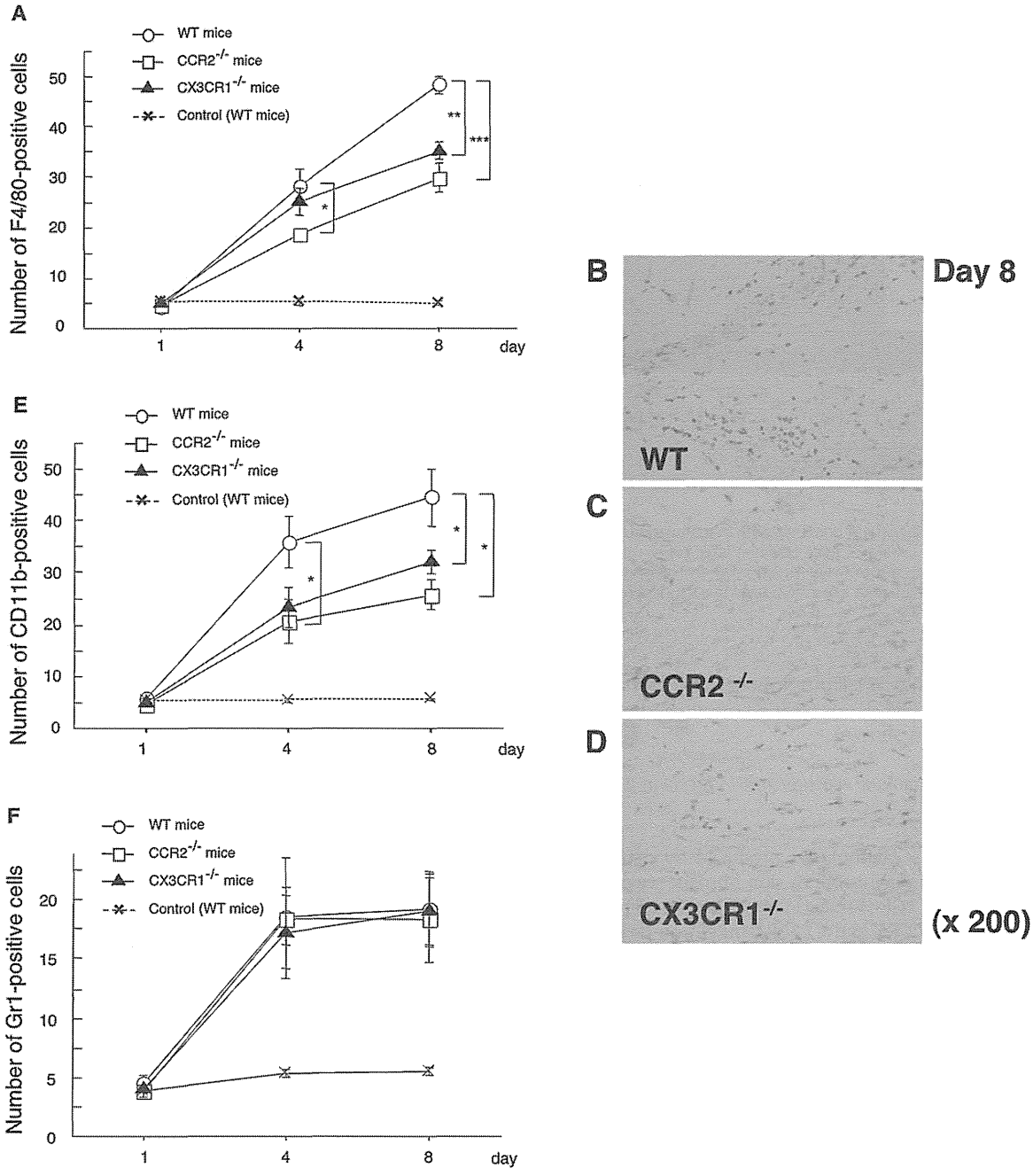

Fig. 5. Kinetics of macrophage recruitment assessed by immunohistochemical analysis using anti-mouse F4/80, CD11b and Gr1 antibody. WT, CCR2$^{-/-}$, and CX3CR1$^{-/-}$ mice were injected with TGF-β and CTGF. Control WT mice were injected with PBS. (A) The total numbers of F4/80-positive cells counted in five high power fields at x200 are shown. (B)–(D) Representative photographs from WT mice (B), CCR2$^{-/-}$ mice (C), and CX3CR1$^{-/-}$ mice (D) on day 8. (E) The total numbers of CD11b-positive cells counted in five high power fields at ×200 are shown. (F) The total numbers of Gr1-positive cells counted in five high power fields at ×200 are shown. Values are the mean ± SEM from 4 to 7 mice in each group. $^{*}p < 0.05$, $^{**}p < 0.005$, $^{***}p < 0.001$.

Fractalkine is expressed by endothelial cells that are activated by proinflammatory cytokines. The fractalkine receptor, CX3CR1, is expressed on mature monocytes, NK cells, and cytotoxic effector T cells. Our data also revealed that serial injections of TGF-β increased fractalkine mRNA and CX3CR1 mRNA expression levels in granulation tissues. Additionally, the blockade of CX3CR1 attenuated macrophage infiltration and skin fibrosis. Furuichi et al. have reported that CX3CR1 deletion attenuates macrophage infiltration as well as late-phase renal interstitial fibrosis and renal function after ischemic-reperfusion injury in a mouse model. In this model, CX3CR1 was found to be expressed mainly in kidney-infiltrating macrophages [30]. Our data linking CX3CR1 to skin fibrosis are consistent with a report stating that CX3CR1 is important for macrophage accumulation in the wound site and that angiogenic and profibrotic macrophage products are reduced in wounded skin in the absence of CX3CR1 [31]. The number of CX3CR1-expressing cells including monocytes were found to be increased in the lesional skin and lung tissues from SSc patients with diffuse cutaneous involvement [24]. Thus, infiltrating F4/80^{+} macrophages are assumed to be mostly CX3CR1 positive. Fractalkine augments the recruitment of CX3CR1-expressing mononuclear cells into the affected tissue of SSc, leading to inflammation and vascular injury. A short-lived CCR2-expressing macrophage subset is actively recruited to inflamed tissues, while

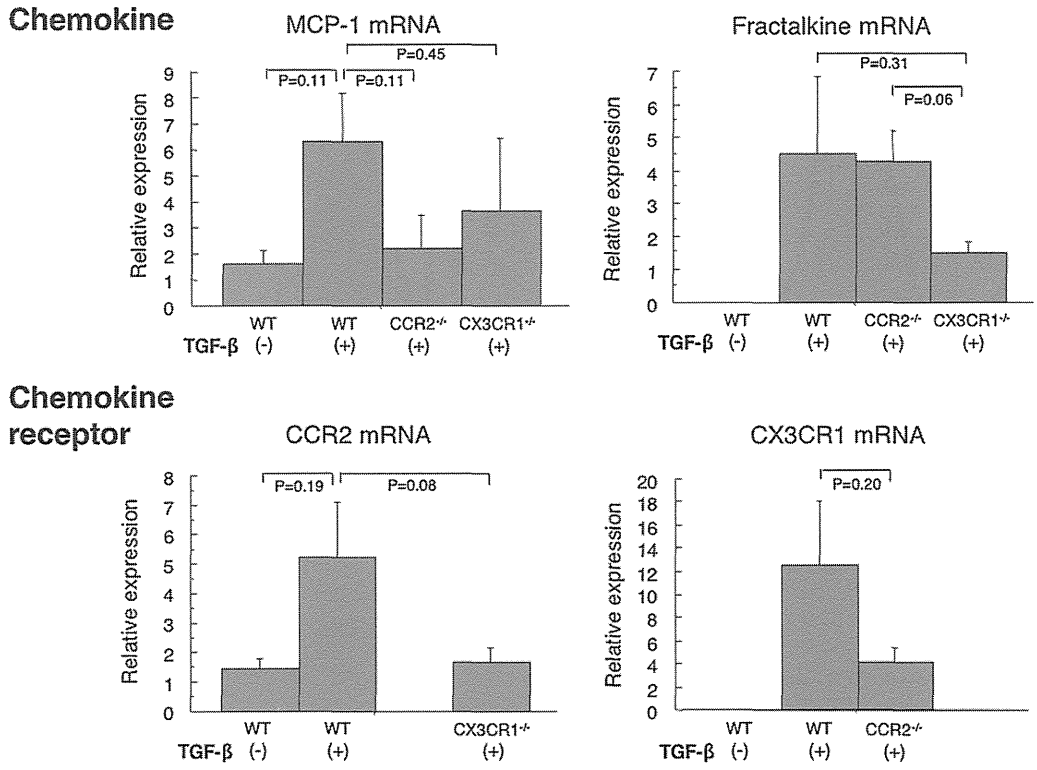

Fig. 6. mRNA levels of chemokines and chemokine receptors in granulation tissues on day 4. The expression levels of MCP-1, fractalkine, CCR2, and CX3CR1 mRNA in granulation tissues from WT mice, CCR2$^{-/-}$ mice, and CXCR1$^{-/-}$ mice 4 days after TGF-β injections were determined by real-time PCR and normalized against the GAPDH mRNA transcript level in each sample. Values are the mean of 4–6 mice in each group. $^{*}p < 0.05$, $^{**}p < 0.005$.

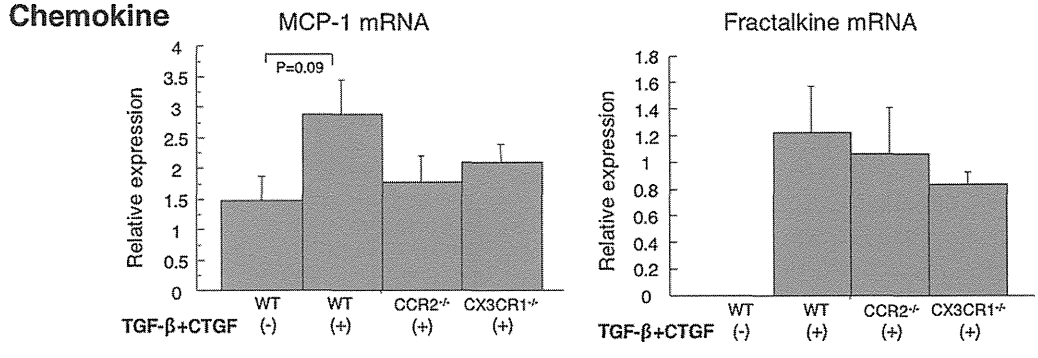

Fig. 7. mRNA levels of chemokines and chemokine receptors in granulation tissues on day 8. The expression levels of MCP-1 and fractalkine mRNA in granulation tissues from WT mice, CCR2$^{-/-}$ mice, and CXCR1$^{-/-}$ mice 8 days after CTGF following TGF-β injections were determined by real-time PCR and normalized against the GAPDH mRNA transcript level in each sample. Values are the mean of 4–6 mice in each group.

the CX3CR1-expressing subset has been characterized as resident in non-inflamed tissue [15]. In the current study, we found that the number of accumulated macrophages was decreased in CCR2$^{-/-}$ mice at day 4, while CX3CR1$^{-/-}$ mice also exhibited moderately reduced macrophage infiltration at day 8. CX3CR1$^{-/-}$ mice also showed less collagen accumulation after both TGF-β and CTGF stimulations, as compared to WT mice.

In vitro, we observed that stimulation with TGF-β significantly augmented fractalkine expression in cultured fibroblasts. To the best of our knowledge, this is the first study to demonstrate the expression of fractalkine in skin fibroblasts. Ruth et al. previously reported increased expression of fractalkine and CX3CR1 in synovial tissue fibroblasts in rheumatoid arthritis (RA) patients as well as in an adjuvant-induced arthritis model in rats [32]. Our data revealed that stimulation with TGF-β significantly augments CTGF mRNA expression in cultured fibroblasts, in the absence of macrophages. Thus, the fractalkine/CX3CR1 pathway may play an important role in the induction of fibrosis via both direct effects on fibroblasts, and indirect effects mediated by cytokine release from CX3CR1-macrophages and leukocytes in the lesional tissues. We have demonstrated that fractalkine was strongly expressed on endothelial cells in the affected skin and lung tissues. Soluble fractalkine levels were significantly elevated in sera and were associated with the existence of digital ischemia, and severity of pulmonary fibrosis [24]. Other studies have shown that Raynaud's phenomenon, a type of ischemia-reperfusion, usually precedes the development of skin sclerosis. Therefore, it is possible that endothelial cell injury caused by recurring ischemia-reperfusion induces inflammatory cell infiltration and cytokine production, leading to the development of tissue fibrosis.

Fractalkine-dependent adhesion of monocytes is greatly enhanced by MCP-1 [33]. Both chemokine pathways may work

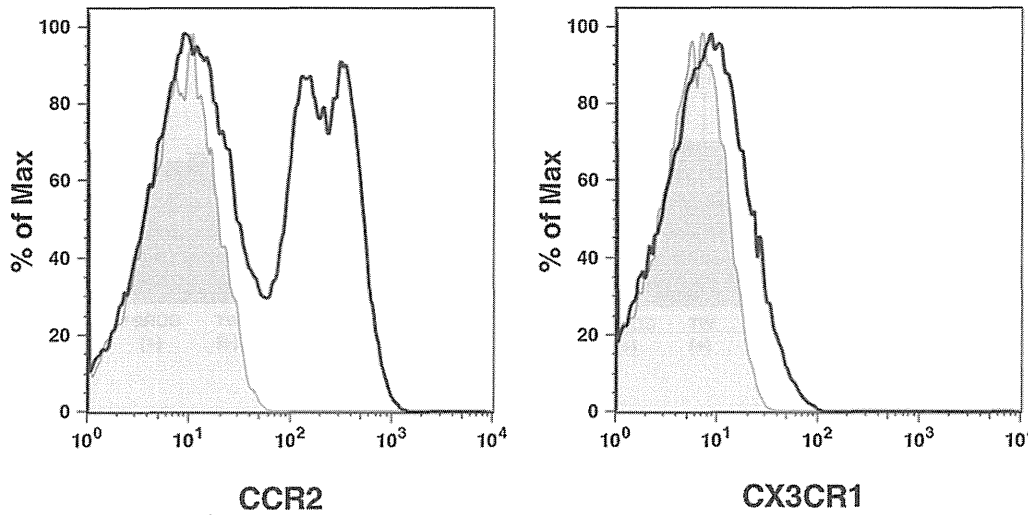

Fig. 8. Representative histograms of CCR2 and CX3CR1 expression on WT macrophages. Bold lines (open regions) in the histogram represent WT CD11b-gaeted cells, and thin lines (shaded regions) in the histogram represent isotype control staining.

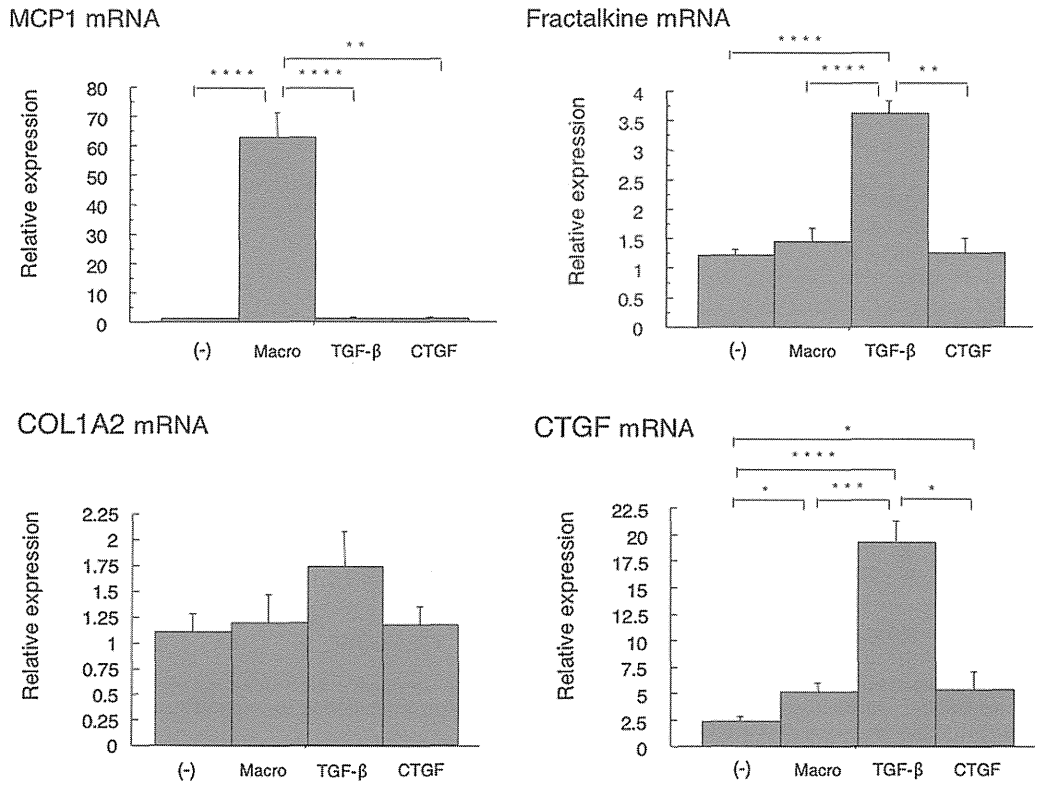

Fig. 9. Chemokines and chemokine receptor mRNA levels from in vitro-cultured fibroblasts. Primary fibroblast cultures were established from dorsal skin of newborn WT mice. TGF-β or CTGF was added to the cell culture medium to a final concentration of 10 ng/ml or 150 ng/ml, respectively. For macrophage-fibroblast cocultures, macrophages (5×10^5 cells per well) were added to the upper wells. Total RNA was isolated from only fibroblasts, and expression levels were determined by real-time PCR and normalized against the GAPDH mRNA transcript level in each sample. Results were obtained from 4 samples in each group. $^{*}p < 0.05$, $^{**}p < 0.01$, $^{***}p < 0.001$, $^{****}p < 0.0005$.

independently and cooperatively to support the firm adhesion of monocytes in vivo. Our data demonstrated that up-regulated transcription of fractalkine and CX3CR1 mRNA in TGF-β-induced fibrosis tended to be reduced by CCR2 deficiency. Also, up-regulated transcription of MCP-1 and CCR2 mRNA in TGF-β-induced fibrosis tended to be reduced by CX3CR1 deficiency.

In summary, fibrosis is a complex process that may involve multiple cytokines and chemokines, which crosstalk with effector cells. MCP-1/CCR2 and fractalkine/CX3CR1 play important roles of the induction and maintenance of fibrosis, likely via differing mechanisms. Therefore, these molecules should be considered as potential therapeutic targets in patients with fibrotic disorders.

Acknowledgments

We thank Yuko Yamada and Masako Matsubara for their technical assistance.

We thank Dr. William Kuziel (University of Texas San Antonio, TX) and Dr. Philip M. Murphy (NIAID, Bethesda, MD) for the gift of $CCR2^{-/-}$ mice and $CX3CR1^{-/-}$ mice.

We thank Nosan Corporation for the gift of Human CTGF.

Appendix A. Supplementary data

Supplementary data associated with this article can be found, in the online version, at http://dx.doi.org/10.1016/j.jdermsci.2012.10.010.

References

[1] Charles C, Clements P, Furst DE. Systemic sclerosis: hypothesis-driven treatment strategies. Lancet 2006;367:1683–91.
[2] Denton CP, Black CM. Targeted therapy comes of age in scleroderma. Trends Immunol 2005;26:596–602.
[3] Varga J, Abraham D. Systemic sclerosis: a prototypic multisystem fibrotic disorder. J Clin Invest 2007;117:557–67.
[4] Varga JA, Trojanowska M. Fibrosis in systemic sclerosis. Rheum Dis Clin North Am 2008;34:115–43. vii.
[5] Jimenez SA, Hitraya E, Varga J. Pathogenesis of scleroderma. Collagen. Rheum Dis Clin North Am 1996;22:647–74.
[6] Distler J, Distler O. Novel treatment approaches to fibrosis in scleroderma. Rheum Dis Clin North Am 2008;34:145–59. vii.
[7] Leroy EC, Smith EA, Kahaleh MB, Trojanowska M, Silver RM. A strategy for determining the pathogenesis of systemic sclerosis. Is transforming growth factor beta the answer? Arthritis Rheum 1989;32:817–25.
[8] Nakerakanti SS, Bujor AM, Trojanowska M. CCN2 is required for the TGF-beta induced activation of Smad1-Erk1/2 signaling network. PLoS ONE 2011;6:e21911.
[9] Takehara K. Hypothesis: pathogenesis of systemic sclerosis. J Rheumatol 2003;30:755–9.
[10] Shinozaki M, Kawara S, Hayashi N, Kakinuma T, Igarashi A, Takehara K. Induction of subcutaneous tissue fibrosis in newborn mice by transforming growth factor beta—simultaneous application with basic fibroblast growth factor causes persistent fibrosis. Biochem Biophys Res Commun 1997;240:292–7.
[11] Mori T, Kawara S, Shinozaki M, Hayashi N, Kakinuma T, Igarashi A, et al. Role and interaction of connective tissue growth factor with transforming growth factor-beta in persistent fibrosis: a mouse fibrosis model. J Cell Physiol 1999;181:153–9.
[12] Chujo S, Shirasaki F, Kawara S, Inagaki Y, Kinbara T, Inaoki M, et al. Connective tissue growth factor causes persistent proalpha2(I) collagen gene expression induced by transforming growth factor-beta in a mouse fibrosis model. J Cell Physiol 2005;203:447–56.
[13] Kraling BM, Maul GG, Jimenez SA. Mononuclear cellular infiltrates in clinically involved skin from patients with systemic sclerosis of recent onset predominantly consist of monocytes/macrophages. Pathobiology 1995;63:48–56.
[14] Kovacs EJ. Fibrogenic cytokines: the role of immune mediators in the development of scar tissue. Immunol Today 1991;12:17–23.
[15] Geissmann F, Jung S, Littman DR. Blood monocytes consist of two principal subsets with distinct migratory properties. Immunity 2003;19:71–82.
[16] Gharaee-Kermani M, Denholm EM, Phan SH. Costimulation of fibroblast collagen and transforming growth factor beta1 gene expression by monocyte chemoattractant protein-1 via specific receptors. J Biol Chem 1996;271:17779–84.
[17] Zhang K, Gharaee-Kermani M, Jones ML, Warren JS, Phan SH. Lung monocyte chemoattractant protein-1 gene expression in bleomycin-induced pulmonary fibrosis. J Immunol 1994;153:4733–41.
[18] Lloyd CM, Minto AW, Dorf ME, Proudfoot A, Wells TN, Salant DJ, et al. RANTES and monocyte chemoattractant protein-1 (MCP-1) play an important role in the inflammatory phase of crescentic nephritis, but only MCP-1 is involved in crescent formation and interstitial fibrosis. J Exp Med 1997;185:1371–80.
[19] Hasegawa M, Sato S, Takehara K. Augmented production of chemokines (monocyte chemotactic protein-1 (MCP-1), macrophage inflammatory protein-1alpha (MIP-1alpha) and MIP-1beta) in patients with systemic sclerosis: MCP-1 and MIP-1alpha may be involved in the development of pulmonary fibrosis. Clin Exp Immunol 1999;117:159–65.
[20] Yamamoto T, Nishioka K. Role of monocyte chemoattractant protein-1 and its receptor, CCR-2, in the pathogenesis of bleomycin-induced scleroderma. J Invest Dermatol 2003;121:510–6.
[21] Moore BB, Paine 3rd R, Christensen PJ, Moore TA, Sitterding S, Ngan R, et al. Protection from pulmonary fibrosis in the absence of CCR2 signaling. J Immunol 2001;167:4368–77.
[22] Okuma T, Terasaki Y, Kaikita K, Kobayashi H, Kuziel WA, Kawasuji M, et al. C-C chemokine receptor 2 (CCR2) deficiency improves bleomycin-induced pulmonary fibrosis by attenuation of both macrophage infiltration and production of macrophage-derived matrix metalloproteinases. J Pathol 2004;204:594–604.
[23] Umehara H, Tanaka M, Sawaki T, Jin ZX, Huang CR, Dong L, et al. Fractalkine in rheumatoid arthritis and allied conditions. Mod Rheumatol 2006;16:124–30.
[24] Hasegawa M, Sato S, Echigo T, Hamaguchi Y, Yasui M, Takehara K. Up regulated expression of fractalkine/CX3CL1 and CX3CR1 in patients with systemic sclerosis. Ann Rheum Dis 2005;64:21–8.
[25] Kuziel WA, Morgan SJ, Dawson TC, Griffin S, Smithies O, Ley K, et al. Severe reduction in leukocyte adhesion and monocyte extravasation in mice deficient in CC chemokine receptor 2. Proc Natl Acad Sci USA 1997;94:12053–58.
[26] Combadiere C, Potteaux S, Gao JL, Esposito B, Casanova S, Lee EJ, et al. Decreased atherosclerotic lesion formation in CX3CR1/apolipoprotein E double knockout mice. Circulation 2003;107:1009–16.
[27] Lopez-De Leon A, Rojkind M. A simple micromethod for collagen and total protein determination in formalin-fixed paraffin-embedded sections. J Histochem Cytochem 1985;33:737–43.
[28] Ishikawa O, Ishikawa H. Macrophage infiltration in the skin of patients with systemic sclerosis. J Rheumatol 1992;19:1202–6.
[29] Gu L, Tseng S, Horner RM, Tam C, Loda M, Rollins BJ. Control of TH2 polarization by the chemokine monocyte chemoattractant protein-1. Nature 2000;404:407–11.
[30] Furuichi K, Gao JL, Murphy PM. Chemokine receptor CX3CR1 regulates renal interstitial fibrosis after ischemia-reperfusion injury. Am J Pathol 2006;169:372–87.
[31] Ishida Y, Gao JL, Murphy PM. Chemokine receptor CX3CR1 mediates skin wound healing by promoting macrophage and fibroblast accumulation and function. J Immunol 2008;180:569–79.
[32] Ruth JH, Volin MV, Haines 3rd GK, Woodruff DC, Katschke Jr KJ, Woods JM, et al. Fractalkine, a novel chemokine in rheumatoid arthritis and in rat adjuvant-induced arthritis. Arthritis Rheum 2001;44:1568–81.
[33] Green SR, Han KH, Chen Y, Almazan F, Charo IF, Miller YI, et al. The CC chemokine MCP-1 stimulates surface expression of CX3CR1 and enhances the adhesion of monocytes to fractalkine/CX3CL1 via p38 MAPK. J Immunol 2006;176:7412–20.

RHEUMATOLOGY

Rheumatology 2013;52:242–251
doi:10.1093/rheumatology/kes258
Advance Access publication 29 September 2012

Original article

Augmented ICOS expression in patients with early diffuse cutaneous systemic sclerosis

Minoru Hasegawa[1], Manabu Fujimoto[1], Takashi Matsushita[1], Yasuhito Hamaguchi[1] and Kazuhiko Takehara[1]

Abstract

Objective. Inducible costimulator (ICOS), expressed on activated T cells, and its ligand, ICOS ligand (ICOSL), expressed on antigen-presenting cells, have been considered a single receptor–ligand pair. Here we investigated the expression of ICOS and ICOSL in patients with SSc.

Methods. ICOS expression on peripheral blood T cells, and ICOSL expression on B cells and macrophages was determined by flow cytometry. Expression of ICOS and ICOSL was assessed by immunohistological staining and real-time PCR of lesional skin.

Results. ICOS expression levels were specifically increased on both peripheral blood memory T cells and Tregs from early dcSSc patients compared with those from healthy controls. Mean ICOSL expression on B cells or macrophages was comparable between SSc patients and healthy controls. ICOS-expressing T cells, ICOSL-expressing macrophages and mRNA levels of ICOS and ICOSL were increased in the lesional skin of patients with early dcSSc. *In vitro* ICOS costimulation enhanced production of IFN-γ, IL-4 and IL-17A from T cells in SSc patients *vs* normal controls. Soluble ICOS levels were significantly increased in SSc patients and were negatively associated with the presence of ACAs and positively associated with CRP values. Serum levels of soluble ICOS were more closely associated with clinical features compared with levels of soluble IL-2 receptor.

Conclusion. Augmented ICOS signalling may contribute to the pathogenesis of SSc during early progressive disease. Soluble ICOS levels may be used as a serum marker for the activity and severity of SSc.

Key words: systemic sclerosis, scleroderma, ICOS, ICOSL, T cell, B cell, macrophage, cytokine, biomarker, sIL-2R.

SCIENCE

Introduction

SSc is a CTD characterized by tissue fibrosis in the skin and internal organs. A growing body of evidence suggests that overproduction of extracellular matrix components by activated fibroblasts results from complex interactions between endothelial cells, leucocytes and fibroblasts via a number of mediators, including cytokines [1–4].

Inducible costimulator (ICOS) is the third member of the CD28 family of costimulatory molecules, and is induced on the cell surface following T-cell activation [5–7]. ICOS ligand (ICOSL) (also called B7-H2, B7h, B7RP-1, LICOS and GL50), the unique ligand of ICOS, is weakly expressed on antigen-presenting cells in the steady state and is up-regulated after activation of these cells [6, 8]. Originally it was reported that the ICOS–ICOSL pathway promotes T-cell activation, differentiation and effector responses, and T-cell-dependent B-cell responses. ICOS-mediated costimulation of T cells leads predominantly to the production of effector cytokines such as IL-4 and IL-10, and to a lesser extent, IL-2, IFN-γ and TNF-α [9], thereby playing a more important role in Th2 responses than Th1 responses [5, 10–12]. However, recent studies have demonstrated that ICOS influences the expansion of follicular T cells, Th17 cells and Tregs [13–15]. Therefore it has been suggested that ICOS–ICOSL signalling is most critical for the survival or expansion of T cells rather than T-cell differentiation.

[1]Department of Dermatology, Kanazawa University Graduate School of Medical Science, Kanazawa, Ishikawa, Japan.

Submitted 23 January 2012; revised version accepted 10 August 2012.

Correspondence to: Minoru Hasegawa, Department of Dermatology, Kanazawa University Graduate School of Medical Science, 13-1 Takaramachi, Kanazawa, Ishikawa 920-8641, Japan.
E-mail: minoruha@derma.m.kanazawa-u.ac.jp

There are numerous reports regarding the roles of ICOS–ICOSL signalling in various animal disease models, including autoimmunity, allergy, infectious diseases, tumour immunity and transplantation [16–19]. Overexpression of ICOS on $CD4^+$ and $CD8^+$ T cells has been reported in patients with SLE [20, 21]. In addition, we reported previously that ICOS and ICOSL affect inflammation and fibrosis in bleomycin-induced skin and lung fibrosis, a model of SSc [22]. However, there were no reports regarding ICOS or ICOSL in patients with SSc. In this study we addressed this deficiency by investigating the expression of ICOS and ICOSL in patients with SSc.

Materials and methods

Patients and clinical assessments

All patients fulfilled the SSc criteria proposed by the ACR [23]. Patients were grouped into lcSSc and dcSSc according to the degree of skin involvement, based on the classification system proposed by LeRoy *et al*. [24]. The dcSSc patients were further divided into early dcSSc (disease duration <3 years) and intermediate/late dcSSc (disease duration >3 years), as proposed by Medsger [25].

The presence of disease-specific autoantibodies was determined by immunoprecipitation. Complete medical histories, physical examinations and laboratory tests were conducted on all patients. The degree of skin involvement was determined according to the modified Rodnan skin thickness score, as described elsewhere [26]. Organ system involvement was defined as described previously [27]. The study was approved by the Ethical Review Board of Kanazawa University. Informed consent was obtained from study participants.

Measurement of serum soluble ICOS levels

Serum levels of soluble ICOS (sICOS) were measured in duplicate with a specific sandwich ELISA kit (Uscn Life Science Inc., Wuhan, China), according to the manufacturer's protocol.

Measurement of serum soluble IL-2 receptor levels

Serum levels of soluble IL-2 receptor (sIL-2R) were measured in duplicate with a specific sandwich ELISA kit (BioVendor Inc., Karasek, Czech Republic), according to the manufacturer's protocol.

Flow cytometric analysis

Heparinized blood samples were collected. Three- or four-colour analysis was performed with a combination of APC-Cy7, FITC, Pacific blue, PE, PE-Cy7 or PerCP-conjugated anti-ICOS antibody (Ab) (Biolegend, San Diego, CA, USA), anti-ICOSL Ab (Biolegend), anti-CD4 Ab (BD Biosciences, San Jose, CA, USA), anti-CD8 Ab (BD Biosciences), anti-CD14 Ab (BD Biosciences), anti-CD19 Ab (BD Biosciences), anti-CD25 Abs (Beckman Coulter, Brea, CA, USA), anti-CD45RO Abs (BD Biosciences), anti-CD69 Abs (Beckman Coulter), anti-CD127 Abs (BD Biosciences) or anti-HLA-DR Abs (Beckman Coulter), as reported previously [22]. FoxP3 staining was performed using intracellular fixation and staining procedures according to the manufacturer's protocol (eBiosciences, San Diego, CA, USA).

Immunohistochemical staining of ICOS and ICOSL

ICOS and ICOSL expression in the skin were determined by immunohistological staining, as reported previously [22]. The serial tissues of skin were stained with rat anti-CD3 (AbD Serotec, Kidlington, OX, UK), mouse anti-CD20 (Dako Cytomation A/S, Tokyo, Japan) and mouse anti-CD68 (Dako Cytomation A/S) Abs to identify the leucocyte subsets of cells expressing ICOS or ICOSL.

RNA isolation and real-time PCR

Total RNA was isolated from the frozen tissue of skin lesions using Qiagen RNeasy spin columns (Qiagen Ltd, Crawley, SXW, UK). Total RNA from each sample was reverse-transcribed into cDNA. Expression of ICOS and ICOSL was analysed using a real-time PCR quantification method (Applied Biosystems, Foster City, CA, USA), as reported previously [22].

T-cell costimulation

Purified $CD4^+$ (2×10^5/well) T cells from each SSc patient and healthy subject were cultured in 96-well, flat-bottomed plates pre-coated with anti-CD3 Ab (12-F6, 3 μg/ml; eBioscience) plus anti-CD28 (CD28.6, 5 μg/ml; eBioscience), anti-ICOS (C398.4A, 5 μg/ml; eBioscience) or hamster IgG (isotype control, 5 μg/ml; eBioscience) for 48 h at 37°C. Each specimen was stimulated in triplicate wells. The supernatants were used for cytometric beads array (BD Biosciences) for cytokine detection.

Statistical analysis

Statistical analyses were performed using Student's *t*-test for comparison of sample means between two groups. For comparisons of more than two groups, one-way analysis of variance with Bonferroni *post hoc* test was used. The Pearson product–moment correlation coefficient was used to examine the relationship between two continuous variables. Multiple regression analysis was also performed in some situations. *P*-values <0.05 were considered to be statistically significant. All values are reported as the mean (S.D.).

Results

Serum sICOS levels

Serum samples were obtained from 68 Japanese patients with SSc and 20 healthy age- and sex-matched volunteers. We evaluated the association between sICOS levels and clinical disease features (Table 1). Twenty healthy age- and sex-matched volunteers served as normal controls [16 women and 4 men, average age 47.8 (16.1) years]. Serum sICOS levels were significantly higher in all patients with SSc or in each SSc subset than in healthy controls ($P < 0.01$; Fig. 1A). Patients with early dcSSc had serum sICOS levels that were significantly higher than those in patients with lcSSc ($P < 0.05$).

Table 1 The profile and clinical features of SSc patients

Clinical parameter	Number (%) of patients, unless otherwise indicated
Female:male	53 (77.9):15 (22.1)
lcSSc	34 (50.0)
dcSSc	34 (50.0)
Early dcSSc	21 (30.9)
Intermediate/late dcSSc	13 (19.0)
Age, mean (S.D.), years	51.3 (11.7)
Disease duration, mean (S.D.), years	4.3 (5.3)
Modified Rodnan total skin thickness score, mean (S.D.), points	12.3 (10.6)
ILD	38 (55.9) (8 lcSSc and 30 dcSSc)
Pulmonary arterial hypertension	4 (5.9)
Oesophagus	32 (47.0)
Heart	1 (1.5)
Kidney	1 (1.5)
Joint	11 (16.2)
Muscle	4 (5.9)
ACAs	22 (32.4)
Anti-topo I Ab	22 (32.4)
Anti-RNA polymerases	1 (1.5)
Anti-U1 RNP Ab	1 (1.5)
Anti-U3 RNP Ab	1 (1.5)
Elevated CRP (>0.05 mg/dl)	6 (8.8)
Elevated ESR (>20 mm/h)	28 (41.2)
%VC, mean (S.D.)	100.1 (18.6)
$\%DL_{CO}$, mean (S.D.)	65.3 (15.5)
CS therapy	28 (41.2)
CYC therapy	2 (2.9)

DL_{CO}: diffusion lung capacity for carbon monoxide; %VC: percentage vital capacity.

Patients with SSc with interstitial lung disease (ILD) had sICOS levels higher than those without ILD, although this increase was not statistically significant. Patients with elevated CRP exhibited significantly higher sICOS levels than in patients with normal CRP levels ($P < 0.05$). Patients without ACAs showed significantly higher sICOS levels than patients with the Abs ($P < 0.05$), although the existence of anti-topo I Ab did not significantly affect the sICOS levels. Other clinical or laboratory factors did not significantly affect sICOS levels. We also performed multiple regressions using a stepwise method that specified the α-level for either adding or removing a regression of 0.15. Among various clinical or laboratory parameters described above, the existence of ACA ($P = 0.01$) and elevated CRP ($P = 0.04$) was determined as predicting factors. As a result, the multiple regression equation predicting sICOS is 1011.8 + ACA ('−' → +98.9, '+' → −98.9) + elevated CRP ('−' → −204.9, '+' → +204.9) [R^2 (determination coefficient) = 0.39, $P < 0.01$, RMSE (root mean square error) = 270.0].

The levels of sICOS could be non-specifically elevated as negative feedback of T-cell activation like sIL-2R, a representative serum marker of T-cell activation. Therefore, serum levels of sIL-2R were also measured in the same serum samples for comparison (Fig. 1B). Although serum sIL-2R levels were elevated in patients with SSc compared with healthy controls, the difference was not statistically significant. Among each disease subset, early dcSSc or lcSSc showed increased sIL-2R levels compared with normal controls, but the differences were not significant. The sIL-2R levels were not significantly associated with any clinical or laboratory features. Moreover, the association between sICOS levels and sIL-2R levels was not significant in patients with SSc ($r = 0.18$, $P = 0.14$). Therefore serum levels of sICOS were more closely associated with clinical features of SSc compared with serum levels of sIL-2R. Thus sICOS was significantly increased in patients with SSc, especially early dcSSc, and was inversely associated with the existence of ACAs.

ICOS expression on peripheral blood mononuclear cell in patients with SSc

Expression levels of ICOS and ICOSL by peripheral blood mononuclear cells (PBMCs) were examined by flow cytometry in more than six patients selected at random from each SSc subgroup (early dcSSc, intermediate/late dcSSc, lcSSc) (Table 2 and Fig. 2). Since the expression levels of this surface marker exhibited slight variability between experiments even in the same healthy controls, results are reported as the percentage of each surface marker in patients *vs* that of the same healthy control ($n = 3$) in each assay. Bulk $CD4^+$ T cells from patients with early dcSSc exhibited 37% higher mean ICOS expression levels than those from normal controls. ICOS expression on memory ($CD45RO^+$) $CD4^+$ T cells was significantly elevated (42%) in early dcSSc patients compared with normal controls. Mean ICOS expression on bulk $CD8^+$ T cells was significantly increased by 18% in patients with early dcSSc compared with controls. ICOS expression on memory ($CD45RO^+$) $CD8^+$ T cells was significantly elevated at 24% in early dcSSc patients compared with normal controls.

Tregs are commonly identified by CD25 (IL-2Rα) surface expression and/or intracellular expression of the FoxP3 transcription factor. Tregs are also characterized by low CD127 (IL-7Rα) expression [28], although $CD25^+FoxP3^+$ T cells and $CD25^+CD127^-$ T cells may represent different Treg populations [29, 30]. Mean ICOS expression on Tregs, defined as either $CD4^+CD25^+FoxP3^+$ or $CD4^+CD25^+C127^-$, was increased by 101% and 54%, respectively, in patients with early dcSSc compared with controls. The ICOS expression levels of each T cell subset from lcSSc were not significantly different from normal controls.

Expression levels of T-cell activation markers were also assessed and the association with ICOS expression was evaluated (Table 2). In general, expression levels of CD25, CD69 and HLA-DR on $CD4^+$ or $CD8^+$ T cells were significantly elevated in each SSc subset (early dcSSc, intermediate/late dcSSc and lcSSc) compared with normal controls. In patients with SSc, ICOS expression levels

FIG. 1 Levels of (**A**) sICOS and (**B**) sIL-2R in serum samples from patients with SSc and healthy controls (CTL).

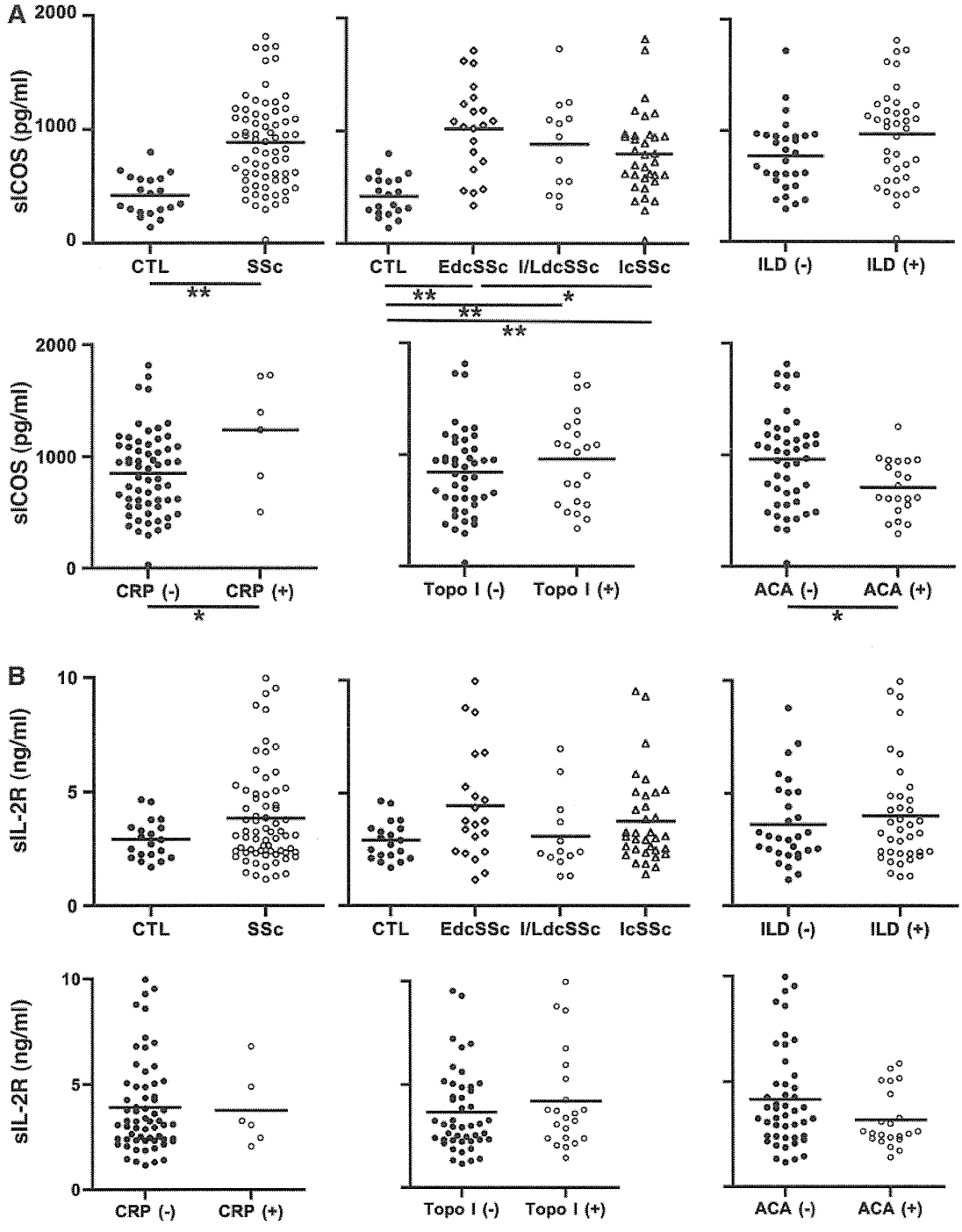

Serum sICOS and sIL-2R levels were also compared with respect to each clinical factor. Levels of sICOS and sIL-2R were determined by sandwich ELISA. Bars show the group means. $^{*}P < 0.05$ and $^{**}P < 0.01$. EdcSSc: early dcSSc; l/LdcSSc: intermediate and late dcSSc.

were significantly associated with that of HLA-DR on $CD4^+$ T cells and $CD8^+$ T cells ($r = 0.49$, $P = 0.008$ and $r = 0.72$, $P = 0.008$, respectively). However, there were no significant associations between ICOS expression levels and expression levels of CD25 or CD69 on $CD4^+$ and $CD8^+$ T cells in patients with SSc (data not shown). These findings indicate that increased ICOS expression on T cells may just be reflecting T-cell activation, but are more specifically increased in patients with early dcSSc compared with expression levels of other T-cell activation

TABLE 2 Expression levels of ICOS and ICOSL on each leucocyte subset in SSc subgroups

Leucocyte subset	Early dcSSc ($n=8$)	Intermediate/late dcSSc ($n=10$)	lcSSc ($n=6$)
ICOS on $CD4^+$ cells	137 (15)**	102 (11)	101 (23)
ICOS on $CD4^+CD45RO^+$ cells	142 (18)**	121 (18)*	94 (17)
ICOS on $CD4^+CD25^+FoxP3^+$ cells	201 (46)**	113 (51)	106 (13)
ICOS on $CD4^+CD25^+CD127^-$ cells	154 (23)**	144 (40)*	112 (64)
ICOS on $CD8^+$ cells	118 (19)*	125 (22)*	95 (15)
ICOS on $CD8^+CD45RO^+$ cells	124 (17)*	136 (28)*	103 (12)
ICOSL on $CD19^+$ cells	117 (29)	99 (24)	94 (24)
ICOSL on $CD14^+$ cells	120 (37)	98 (12)	94 (20)
CD25 on $CD4^+$ cells	157 (28)**	147 (17)**	128 (9)*
CD69 on $CD4^+$ cells	127 (15)*	122 (11)*	129 (16)*
HLA-DR on $CD4^+$ cells	174 (43)**	161 (15)**	177 (19)**
CD25 on $CD8^+$ cells	108 (5)	98 (7)	106 (6)
CD69 on $CD8^+$ cells	149 (18)*	114 (12)	145 (19)*
HLA-DR on $CD8^+$ cells	127 (18)*	154 (14)*	128 (32)

Expression levels of ICOS and ICOSL were assessed by flow cytometry. Results [mean (S.D.)] are reported as the percentage of each surface marker in patients *vs* that of the same healthy control ($n=3$) in each assay. *$P<0.05$ *vs* normal controls, **$P<0.01$ *vs* normal controls.

markers. Thus expression levels of ICOS were significantly increased on peripheral blood memory T cells and Tregs in patients with early dcSSc.

ICOSL expression on antigen-presenting cells in SSc samples

We next examined ICOSL expression on B cells and macrophages from SSc patient peripheral blood samples (Table 2 and Fig. 2). The mean ICOSL expression on $CD19^+$ B cells was not significantly different between each SSc subset and normal controls. We then examined ICOSL expression on $CD14^+$ macrophages and found this to be comparable between SSc patients and normal controls. Overall the ICOSL levels on B cells or macrophages were not significantly different between each SSc subset.

Immunohistochemical examination of ICOS- and ICOSL-expressing cells

Biopsy samples were taken from the lesional skin (dorsal aspect of the mid-forearm) of eight females in each SSc subgroup. In the affected skin tissue from patients with early dcSSc, a considerable number of ICOS-expressed mononuclear cells were found around the small vessels (Fig. 3A and C). $ICOS^+$ cells were less commonly found in affected skin tissue from patients with intermediate/late dcSSc or lcSSc. $ICOS^+$ cells were sparse by immunohistochemical staining of normal control skin tissue. Although the frequency of ICOS-positive cells among mononuclear cells was higher in patients with early dcSSc [75 (10%)] compared with that in normal controls and patients with late dcSSc or lcSSc, the difference was not statistically significant (Fig. 3B). Most $CD3^+$ T cells were considered as expressing ICOS by immunohistochemical staining of serial sections (data not shown).

Although there were some variations between patients, moderate numbers of ICOSL-expressed mononuclear cells were detected around the small vessels of affected skin from patients with early dcSSc (Fig. 3A and C). $ICOSL^+$ cells were modestly found in affected skin tissue from patients with intermediate/late dcSSc and lcSSc. $ICOSL^+$ cells were only sparsely detected by immunohistochemical staining of normal control skin tissue. Although the frequency of ICOSL-expressed cells among mononuclear cells was higher in early dcSSc patients [18 (6%)] than in normal controls and patients with late dcSSc or lcSSc, the difference was not statistically significant (Fig. 3B). Most of the $ICOSL^+$ cells were considered as monocytes/macrophages morphologically and by immunostaining with anti-CD68 Ab in serial sections (data not shown). $CD20^+$ B cells were very few in the skin tissues from patients with SSc and normal controls (data not shown). Thus infiltration of $ICOS^+$ cells and $ICOSL^+$ cells was increased in the affected skin from patients with early dcSSc.

ICOS and ICOSL mRNA expression in the skin

Next we examined the expression of ICOS and ICOSL mRNA in the lesional skin of more than eight early dcSSc patients and normal control skin by real-time PCR (Fig. 3D). ICOS mRNA levels in patients with early dcSSc were significantly higher in the lesional skin than those in healthy control subjects ($P<0.05$). Additionally, ICOSL mRNA also showed a significant elevation in the skin of early dcSSc patients compared with healthy subjects ($P<0.05$). Thus mRNA expression levels of ICOS and ICOSL were augmented significantly in the skin of patients with early dcSSc, although the elevation was not so dramatic despite the marked increase of ICOS- or ICOSL-expressed mononuclear cells in the lesional skin by immunohistochemical staining.

FIG. 2 Expression of ICOS and ICOSL on leucocyte subpopulations from patients with early dcSSc and normal controls.

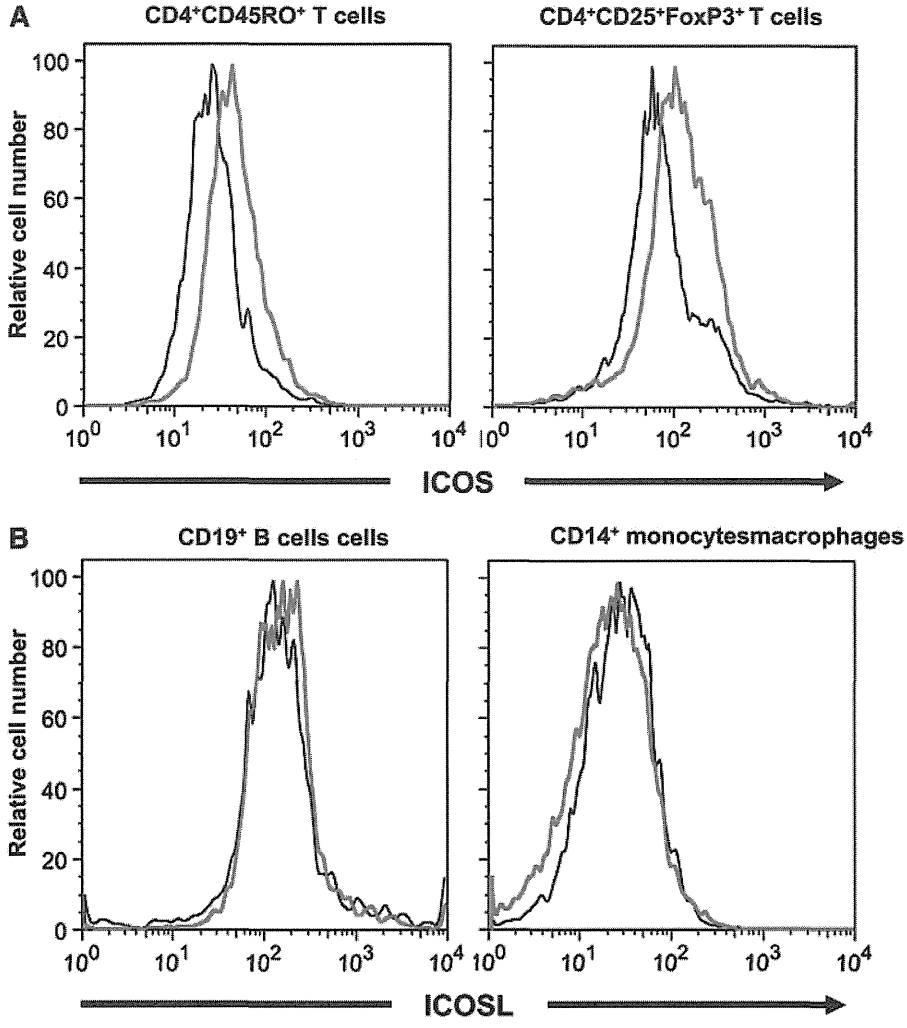

Expression levels were assessed by three- or four-colour immunofluorescent staining and flow cytometric analysis. All samples were stained and analysed sequentially by flow cytometry using the same instrument settings. (**A**) Representative expression of ICOS on $CD4^+CD45RO^+$ memory T cells and $CD4^+CD25^+FoxP3^+$ Tregs from patients with early dcSSc (bold red line) and normal controls (thin line). (**B**) Representative expression of ICOSL on $CD19^+$ B cells and $CD14^+$ monocytes from patients with early dcSSc (bold red line) and normal controls (thin line). Relative fluorescence intensity is shown on a log scale.

ICOS costimulation on T cells

As expression levels of ICOS were up-regulated in early dcSSc patients, we examined the effects of *ex vivo* ICOS ligation on T cells from early dcSSc patients. Purified $CD4^+$ T cells from the peripheral blood of early dcSSc patients and age- and sex-matched healthy controls ($n = 5$) were costimulated with either anti-ICOS Ab or anti-CD28 Ab. The supernatants were used for cytometric beads array evaluation of cytokine production (Fig. 4). CD28 costimulation significantly increased the production of IL-2, IL-4 and IL-17A in both normal controls and SSc patients, and the levels were similar between controls and SSc patients. On the other hand, ICOS costimulation significantly augmented the production of IFN-γ, IL-4 and IL-17A in SSc patients but not in normal controls. However, CD28 or ICOS costimulation did not significantly affect the production of TNF-α, IL-6 and IL-10. Thus ICOS costimulation induced production of pro-inflammatory (IFN-γ and IL-17A) and pro-fibrogenic cytokines (IL-4) from $CD4^+$ T cells from early dcSSc patients.

Discussion

In the present study, the expression levels of ICOS on peripheral blood T cells were found to be significantly elevated in patients with early dcSSc. Additionally, mRNA expression levels of ICOS and ICOSL were augmented in the affected skin of early dcSSc patients.

FIG. 3 Expression of ICOS and ICOSL in skin tissue from patients with SSc.

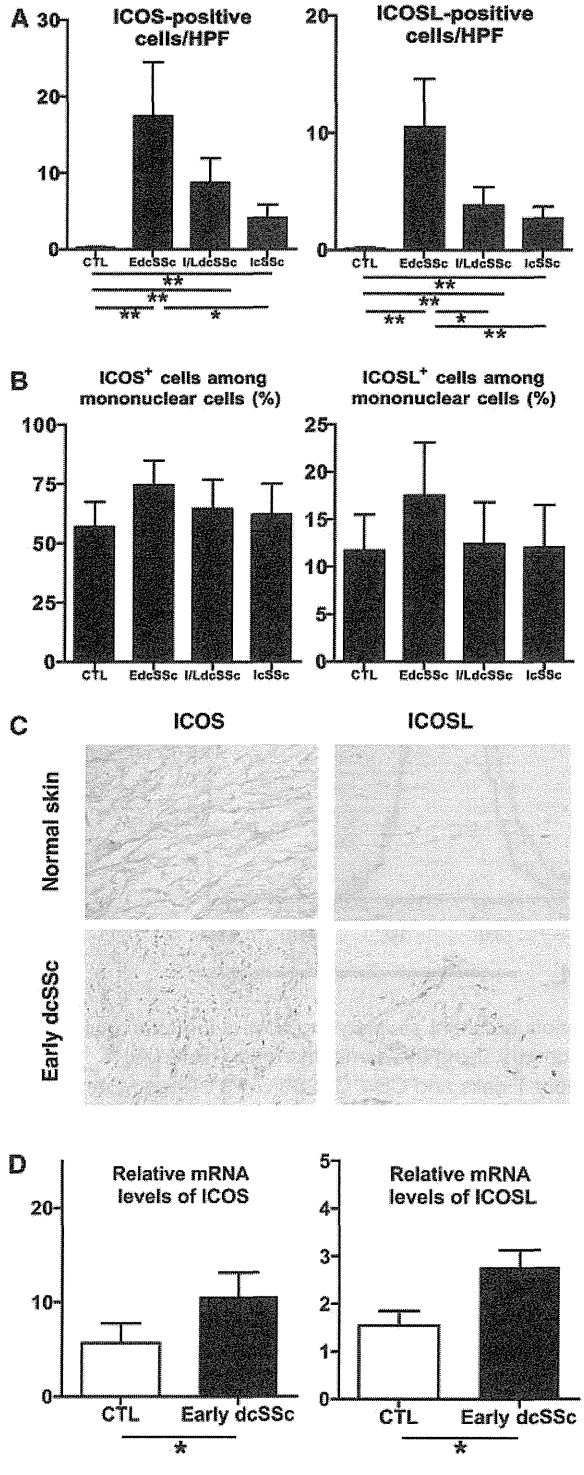

(**A**) Number [mean (S.D.)] of ICOS- or ICOSL-positive cells in normal skin tissue (CTL) and skin tissue from early dcSSc (EdcSSc), intermediate/late dcSSc (l/LdcSSc) and lcSSc ($n = 5$). (**B**) Frequency [(mean (S.D.)] of ICOS- or ICOSL-positive cells among mononuclear cells in each group. (**C**) Representative immunohistological pictures in normal skin tissues and skin tissues from EdcSSc patients with rapidly progressing skin sclerosis. Magnification ×200. (**D**) ICOS and ICOSL mRNA expression in affected skin from patients with EdcSSc and CTL ($n = 8$). Real-time PCR was used to quantify the expression of mRNA in skin samples obtained from patients with EdcSSc and CTL. $^{*}P < 0.05$ and $^{**}P < 0.01$.

Ex vivo ICOS costimulation of $CD4^+$ T cells from SSc patients led to specific induction of pro-inflammatory and pro-fibrogenic cytokines. We found that serum sICOS levels were significantly increased in patients with SSc, and were inversely associated with the existence of ACAs and positively associated with elevated CRP. These findings suggest that augmented ICOS–ICOSL signalling contributes to the development of SSc via cytokine production from T cells, especially in the early progressive stage of disease. Furthermore, sICOS levels may be a useful biomarker for evaluating the disease activity and/or severity of SSc.

The current study demonstrates that expression of ICOS is significantly increased on memory T cells from SSc patients. ICOS-expressing T cells and ICOS mRNA were both significantly increased in the lesional skin from SSc patients. There are several reports regarding ICOS expression in other inflammatory diseases. One previous study demonstrated that ICOS expression is increased on peripheral $CD4^+$ as well as $CD8^+$ T cells in patients with SLE [20, 21]. Regarding ICOS expression on specific T-cell subsets, the finding of ICOS overexpression on $CD4^+$ and $CD8^+$ memory T cells in patients with active SLE, but not inactive SLE, is similar to our findings in SSc patients [31]. ICOS overexpression on peripheral $CD4^+$ and $CD8^+$ T cells has been shown to contribute to dysregulated T-cell proliferation, T-cell activation and pathogenic Ab production in SLE *in vitro* [21]. Another report demonstrated that ICOS expression is elevated on $CD4^+$ T cells and contributes to the production of IFN-γ, IL-17 and TNF-α from PMBCs of Behçet's disease patients with uveitis [32]. In addition, expression of ICOS on T cells was increased in SF of RA patients [33]. These findings highlight the importance of the ICOS signalling pathway in a variety of autoimmune or inflammatory diseases.

By contrast, a down-regulation of ICOSL has been reported on peripheral blood memory B cells in patients with SLE [20]. *In vitro* experiments indicate that ICOSL down-regulation on B cells is a signature of recent interaction with ICOS-expressing T cells [20]. In our study, ICOSL expression levels on peripheral blood B cells or macrophages from SSc patients were not significantly different from those of normal controls. We previously reported that ICOS-deficient mice show markedly increased ICOSL expression on splenic macrophages and B cells, whereas ICOSL-deficient mice exhibit striking increases in ICOS expression on splenic T cells [22]. Therefore it is possible that increased ICOS expression on T cells in SSc patients

FIG. 4 Cytokine production from $CD4^+$ T cells by ICOS costimulation.

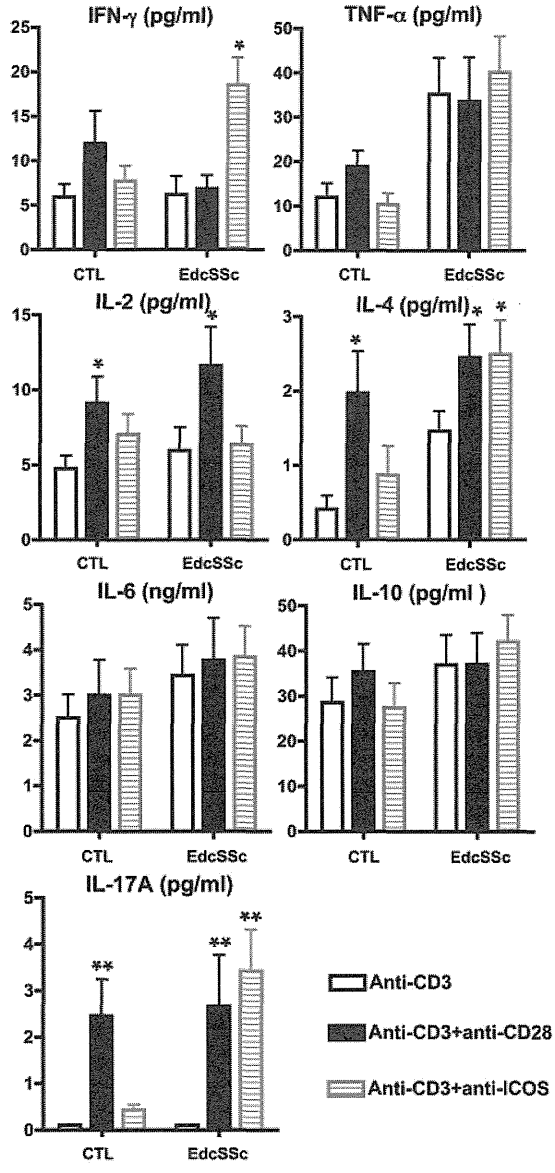

Peripheral $CD4^+$ T cells from early dcSSc (EdcSSc) patients and normal controls (CTL) were stimulated with pre-coated anti-CD3 Ab plus anti-CD28 Ab, anti-ICOS Ab or control IgG for 48 h. Supernatants were used for cytometric bead array. $^*P < 0.05$ and $^{**}P < 0.01$ *vs* anti-CD3 Ab costimulation.

may down-regulate ICOSL expression on antigen-presenting cells, as found in SLE. Nonetheless, in our present study we found that ICOSL levels were not reduced, and ICOSL-expressing mononuclear cells and mRNA levels of ICOSL were increased in the skin of early dcSSc patients. Therefore increased ICOS expression can enhance ICOS–ICOSL interactions and may affect both ICOS-expressing T cells and ICOSL-expressing B cells and macrophages in SSc.

ICOS is expressed at low levels on resting naïve T cells and is rapidly up-regulated after TCR ligation and CD28 costimulation [9]. ICOS expression can be regulated by signalling molecules activated downstream of TCR engagement and CD28 costimulation, including the Src kinase Fyn and the MAP kinase ERK at the transcription level [34, 35]. ICOS expression can be also regulated by the RING-type ubiquitin ligase family member Roquin at the post-transcriptional level [36, 37]. It is also possible that ICOS expression is differentially regulated in each T-cell lineage [38]. Increased ICOS expression may just be reflecting the activation of T cells. Nonetheless, levels of ICOS expression on T cells were more specifically increased in early dcSSc compared with other activation markers. Therefore increased ICOS expression levels may be contributing to the development of SSc, especially in patients with early dcSSc.

ICOS expression was also increased in Tregs in patients with SSc. This is not surprising since ICOS is expressed on all T cells after activation [39]; thus enhanced ICOS on memory T cells and Tregs probably reflects cellular activation status, indicating that these T cells are continuing to receive antigen receptor and CD28 stimulation *in vivo*. Recent studies have demonstrated that Tregs could also be working as effector cells via production of IL-17A in response to IL-1β and IL-6 [40–42]. It has been reported that the $CD4^+ICOS^+FoxP3^+$ subset of Tregs can be distinguished from other Tregs by the production of effector cytokines in mice [43, 44]. Therefore increased ICOS expression on Tregs in early dcSSc may reflect precursor inflammatory T cells. Under certain conditions they may lose their suppressor functions and convert to effector T cells, as suggested in the case of both active SLE and a murine melanoma model [44, 45]. Thus the net effect of ICOS–ICOSL signalling in host immune responses is probably dependent on the environment, which can lead to seemingly controversial results depending on the disease or disease models being examined [42, 44, 46]. In this study, *in vitro* ICOS costimulation induced the production of IFN-γ, IL-4 and IL-17A from peripheral blood T cells. IL-4 is a representative pro-fibrogenic cytokine, and IFN-γ and IL-17A are pro-inflammatory cytokines, although IFN-γ has anti-pro-fibrogenic effects. Recent studies suggest critical roles of IL-17A in fibrogenic diseases, including SSc [47–49]. Therefore augmented ICOS signalling may be contributing to the development of fibrosis via cytokine production in patients with SSc.

To the best of our knowledge, this study is the first to evaluate sICOS levels in human or animal serum samples. We found that sICOS levels were markedly increased in patients with early dcSSc. While SSc patients with ACA generally show mild symptoms except for pulmonary arterial hypertension, sICOS levels were significantly increased in SSc patients without ACA and SSc patients with elevated CRP. It has been reported that serum levels of sIL-2R reflect the T-cell activation and disease activity or severity in various inflammatory diseases including SSc [50]. However, serum levels of sICOS were more closely associated with clinical features of SSc compared with

serum levels of sIL-2R. The mechanism of shedding and the roles of sICOS remain unknown. Nonetheless, our findings indicate that sICOS levels may be useful as a biomarker of disease activity and severity in SSc patients.

Rheumatology key messages

- ICOS expression on peripheral T cells and the lesional skin is augmented in patients with early dcSSC.
- Soluble ICOS levels may be useful as a serum marker of disease activity and severity in patients with SSc.

Funding: This work was supported by grants-in-aid from the Ministry of Education, Science and Culture of Japan, and funds for Research on Intractable Diseases from the Ministry of Health, Labour and Welfare of Japan.

Disclosure statement: The authors have declared no conflicts of interest.

References

1 Varga J, Abraham D. Systemic sclerosis: a prototypic multisystem fibrotic disorder. J Clin Invest 2007;117:557–67.

2 Gabrielli A, Avvedimento EV, Krieg T. Scleroderma. N Engl J Med 2009;360:1989–2003.

3 Baraut J, Michel L, Verrecchia F, Farge D. Relationship between cytokine profiles and clinical outcomes in patients with systemic sclerosis. Autoimmun Rev 2010;10:65–73.

4 Chizzolini C, Brembilla NC, Montanari E, Truchetet ME. Fibrosis and immune dysregulation in systemic sclerosis. Autoimmun Rev 2011;10:276–81.

5 Hutloff A, Dittrich AM, Beier KC *et al.* ICOS is an inducible T-cell co-stimulator structurally and functionally related to CD28. Nature 1999;397:263–6.

6 Yoshinaga SK, Whoriskey JS, Khare SD *et al.* T-cell co-stimulation through B7RP-1 and ICOS. Nature 1999;402:827–32.

7 Greenwald RJ, Freeman GJ, Sharpe AH. The B7 family revisited. Annu Rev Immunol 2005;23:515–48.

8 Swallow MM, Wallin JJ, Sha WC. B7h, a novel costimulatory homolog of B7.1 and B7.2, is induced by TNFalpha. Immunity 1999;11:423–32.

9 McAdam AJ, Chang TT, Lumelsky AE *et al.* Mouse inducible costimulatory molecule (ICOS) expression is enhanced by CD28 costimulation and regulates differentiation of $CD4^+$ T cells. J Immunol 2000;165:5035–40.

10 Nurieva RI, Chung Y, Hwang D *et al.* Generation of T follicular helper cells is mediated by interleukin-21 but independent of T helper 1, 2, or 17 cell lineages. Immunity 2008;29:138–49.

11 Coyle AJ, Gutierrez-Ramos JC. The role of ICOS and other costimulatory molecules in allergy and asthma. Springer Semin Immunopathol 2004;25:349–59.

12 Lohning M, Hutloff A, Kallinich T *et al.* Expression of ICOS in vivo defines $CD4^+$ effector T cells with high inflammatory potential and a strong bias for secretion of interleukin 10. J Exp Med 2003;197:181–93.

13 Bauquet AT, Jin H, Paterson AM *et al.* The costimulatory molecule ICOS regulates the expression of c-Maf and IL-21 in the development of follicular T helper cells and TH-17 cells. Nat Immunol 2009;10:167–75.

14 Burmeister Y, Lischke T, Dahler AC *et al.* ICOS controls the pool size of effector-memory and regulatory T cells. J Immunol 2008;180:774–82.

15 Akbari O, Freeman GJ, Meyer EH *et al.* Antigen-specific regulatory T cells develop via the ICOS-ICOS-ligand pathway and inhibit allergen-induced airway hyperreactivity. Nat Med 2002;8:1024–32.

16 Rottman JB, Smith T, Tonra JR *et al.* The costimulatory molecule ICOS plays an important role in the immunopathogenesis of EAE. Nat Immunol 2001;2:605–11.

17 Dong C, Juedes AE, Temann UA *et al.* ICOS co-stimulatory receptor is essential for T-cell activation and function. Nature 2001;409:97–101.

18 Kopf M, Coyle AJ, Schmitz N *et al.* Inducible costimulator protein (ICOS) controls T helper cell subset polarization after virus and parasite infection. J Exp Med 2000;192:53–61.

19 Ozkaynak E, Gao W, Shemmeri N *et al.* Importance of ICOS-B7RP-1 costimulation in acute and chronic allograft rejection. Nat Immunol 2001;2:591–6.

20 Hutloff A, Buchner K, Reiter K *et al.* Involvement of inducible costimulator in the exaggerated memory B cell and plasma cell generation in systemic lupus erythematosus. Arthritis Rheum 2004;50:3211–20.

21 Yang JH, Zhang J, Cai Q *et al.* Expression and function of inducible costimulator on peripheral blood T cells in patients with systemic lupus erythematosus. Rheumatology 2005;44:1245–54.

22 Tanaka C, Fujimoto M, Hamaguchi Y *et al.* Inducible costimulator ligand regulates bleomycin-induced lung and skin fibrosis in a mouse model independently of the inducible costimulator/inducible costimulator ligand pathway. Arthritis Rheum 2010;62:1723–32.

23 Subcommittee for Scleroderma Criteria of the American Rheumatism Association Diagnostic and Therapeutic Criteria Committee. Preliminary criteria for the classification of systemic sclerosis (scleroderma). Arthritis Rheum 1980;23:581–90.

24 LeRoy EC, Krieg T, Black C *et al.* Scleroderma (systemic sclerosis): classification, subsets, and pathogenesis. J Rheumatol 1988;15:202–5.

25 Medsger TA. Jr. Systemic sclerosis. In: Clements PJ, Furst DE, eds. Classification, purpose. Philadelphia: Williams & Wilkins, 2004:17–28.

26 Clements P, Lachenbrush P, Seibold J *et al.* Inter and intraobserver variability of total skin thickness score (modified Rodnan TSS) in systemic sclerosis. J Rheumatol 1995;22:1281–5.

27 Steen VD, Powell DL, Medsger TAJ. Clinical correlations and prognosis based on serum autoantibodies in patients with systemic sclerosis. Arthritis Rheum 1988;31:196–203.

28 Liu W, Putnam AL, Xu-Yu Z *et al*. CD127 expression inversely correlates with FoxP3 and suppressive function of human CD4+ T reg cells. J Exp Med 2006;203:1701–11.

29 Klein S, Kretz CC, Krammer PH, Kuhn A. CD127(low/-) and FoxP3(+) expression levels characterize different regulatory T-cell populations in human peripheral blood. J Invest Dermatol 2010;130:492–9.

30 Simonetta F, Chiali A, Cordier C *et al*. Increased CD127 expression on activated $FOXP3^+CD4^+$ regulatory T cells. Eur J Immunol 2010;40:2528–38.

31 Gang C, Jiahui Y, Huaizhou W *et al*. Defects of mitogen-activated protein kinase in ICOS signaling pathway lead to CD4(+) and CD8(+) T-cell dysfunction in patients with active SLE. Cell Immunol 2009;258:83–9.

32 Usui Y, Takeuchi M, Yamakawa N *et al*. Expression and function of inducible costimulator on peripheral blood CD4+ T cells in Behcet's patients with uveitis: a new activity marker? Invest Ophthalmol Vis Sci 2010;51:5099–104.

33 Ruth JH, Rottman JB, Kingsbury GA *et al*. ICOS and B7 costimulatory molecule expression identifies activated cellular subsets in rheumatoid arthritis. Cytometry A 2007;71:317–26.

34 Zamoyska R, Basson A, Filby A *et al*. The influence of the src-family kinases, Lck and Fyn, on T cell differentiation, survival and activation. Immunol Rev 2003;191:107–18.

35 Tan AH, Wong SC, Lam KP. Regulation of mouse inducible costimulator (ICOS) expression by Fyn-NFATc2 and ERK signaling in T cells. J Biol Chem 2006;281:28666–78.

36 Vinuesa CG, Cook MC, Angelucci C *et al*. A RING-type ubiquitin ligase family member required to repress follicular helper T cells and autoimmunity. Nature 2005;435:452–8.

37 Yu D, Tan AH, Hu X *et al*. Roquin represses autoimmunity by limiting inducible T-cell co-stimulator messenger RNA. Nature 2007;450:299–303.

38 Simpson TR, Quezada SA, Allison JP. Regulation of CD4 T cell activation and effector function by inducible costimulator (ICOS). Curr Opin Immunol 2010;22:326–32.

39 Herman AE, Freeman GJ, Mathis D, Benoist C. $CD4^+CD25^+$ T regulatory cells dependent on ICOS promote regulation of effector cells in the prediabetic lesion. J Exp Med 2004;199:1479–89.

40 Voo KS, Wang YH, Santori FR *et al*. Identification of IL-17-producing $FOXP3^+$ regulatory T cells in humans. Proc Natl Acad Sci USA 2009;106:4793–8.

41 Ayyoub M, Deknuydt F, Raimbaud I *et al*. Human memory $FOXP3^+$ Tregs secrete IL-17 ex vivo and constitutively express the T(H)17 lineage-specific transcription factor RORgamma t. Proc Natl Acad Sci USA 2009;106:8635–40.

42 Beriou G, Costantino CM, Ashley CW *et al*. IL-17-producing human peripheral regulatory T cells retain suppressive function. Blood 2009;113:4240–9.

43 Vocanson M, Rozieres A, Hennino A *et al*. Inducible costimulator (ICOS) is a marker for highly suppressive antigen-specific T cells sharing features of TH17/TH1 and regulatory T cells. J Allergy Clin Immunol 2010;126:280–9, 289 e1–7.

44 Fu T, He Q, Sharma P. The ICOS/ICOSL pathway is required for optimal antitumor responses mediated by anti-CTLA-4 therapy. Cancer Res 2011;71:5445–54.

45 Liu Y, Zhu T, Cai G *et al*. Elevated circulating $CD4^+$ $ICOS^+$ $Foxp3^+$ T cells contribute to overproduction of IL-10 and are correlated with disease severity in patients with systemic lupus erythematosus. Lupus 2011;20:620–7.

46 Martin-Orozco N, Li Y, Wang Y *et al*. Melanoma cells express ICOS ligand to promote the activation and expansion of T-regulatory cells. Cancer Res 2010;70:9581–90.

47 Wilson MS, Madala SK, Ramalingam TR *et al*. Bleomycin and IL-1beta-mediated pulmonary fibrosis is IL-17A dependent. J Exp Med 2010;207:535–52.

48 Radstake TR, van Bon L, Broen J *et al*. The pronounced Th17 profile in systemic sclerosis (SSc) together with intracellular expression of TGFbeta and IFNgamma distinguishes SSc phenotypes. PLoS One 2009;4:e5903.

49 Kurasawa K, Hirose K, Sano H *et al*. Increased interleukin-17 production in patients with systemic sclerosis. Arthritis Rheum 2000;43:2455–63.

50 Degiannis D, Seibold JR, Czarnecki M, Raskova J, Raska K Jr. Soluble interleukin-2 receptors in patients with systemic sclerosis. Clinical and laboratory correlations. Arthritis Rheum 1990;33:375–80.

A randomised, double-blind, placebo-controlled trial: intravenous immunoglobulin treatment in patients with diffuse cutaneous systemic sclerosis

K. Takehara[1], H. Ihn[2], S. Sato[3]

[1]Department of Dermatology, Faculty of Medicine, Institute of Medical, Pharmaceutical, and Health Sciences, Kanazawa University, Kanazawa, Japan; [2]Department of Dermatology and Plastic Surgery, Faculty of Life Sciences, Kumamoto University, Kumamoto, Japan; [3]Department of Dermatology, Graduate School of Medicine, University of Tokyo, Tokyo, Japan.

Kazuhiko Takehara, MD
Hironobu Ihn, MD
Shinichi Sato, MD
and members of the GB-0998 Study Group

Please address correspondence and reprint requests to:
Kazuhiko Takehara, MD,
Department of Dermatology,
Faculty of Medicine,
Institute of Medical, Pharmaceutical, and Health Sciences,
Kanazawa University,
13-1 Takara-machi, Kanazawa,
920-8641 Ishikawa, Japan.
E-mail: takehara@med.kanazawa-u.ac.jp

Received on January 21, 2013; accepted in revised form on February 20, 2013.

Clin Exp Rheumatol 2013; 31 (Suppl. 76): S151-S156.

Key words: systemic sclerosis, IVIG, DBT

Competing interests: K. Takehara is a clinical consultant of this trial; the other co-authors have declared no competing interests.

ABSTRACT

Objectives. *This paper aims to investigate the efficacy of intravenous immunoglobulin (IVIG) for skin sclerosis in diffuse cutaneous systemic sclerosis (dcSSc) by a randomised, double-blind, placebo-controlled, multicentre trial (DBT) with subsequent long-term observational and readministration studies.*

Methods. *In DBT, IVIG (400mg/kg/day for 5 consecutive days: a single course) or placebo (P) was intravenously administered to 63 dcSSc patients of 17 medical institutions in Japan, and changes in the modified Rodnan skin thickness score (MRSS) 12 weeks after administration or at discontinuation were compared as a primary endpoint. Patients with a 5-point or more improvement in the MRSS were continuously observed (long-term observational study), whereas IVIG was administered to those with less than a 5-point improvement (readministration study).*

Results. *In DBT, changes in the MRSS (mean±SD) were -3.3±4.2 and -4.2±4.6 in IVIG and P groups, respectively, and were not significantly different. Non-responder patients were subsequently subjected to the readministration study, and the change in the MRSS (LS-mean±SEM) at 60 weeks after the first administration was -8.3±1.0 in the IVIG → IVIG (GG) group treated with two courses of IVIG administration and -4.1±1.1 in the P → IVIG (PG) group treated with a single course of IVIG administration. The GG group represented a significant improvement in the MRSS against the PG group (p=0.0040).*

Conclusion. *Although the primary endpoint was not achieved in DBT, repeated administration of IVIG for two courses may be effective for skin sclerosis in dcSSc. Further investigation by the administration of plural courses will be necessary.*

Introduction

Systemic sclerosis (scleroderma or SSc) is a disease characterised by fibrosis of the skin and visceral organs, and extracellular matrix, mainly type I and type III collagen, is excessively deposited. The cause is unclear, but autoimmune phenomena, collagen metabolism, overproduction of growth factors and cytokines, vascular disorders, hereditary backgrounds, and environmental factors are considered to be entangled in a complex way to form the pathology. The disease is classified as an autoimmune disease because autoantibodies against cell nuclear components, such as topoisomerase I and centromere, are frequently detected (1, 2). In diffuse cutaneous SSc (dcSSc), skin sclerosis expands toward proximal regions of the elbow and knee and acutely aggravates, and pulmonary, renal, and myocardial impairments occur frequently.

Since fibrotic lesions in SSc are less reversible, the main objective of treatment is set at the prevention of organ disorders and inhibition of progression when impairments are already present. Many agents have been investigated as therapeutic drugs to inhibit the progression of SSc, although no drug has demonstrated clear efficacy for the improvement of skin sclerosis by a multicentre, randomised, double-blind, controlled study (3-7).

Intravenous immunoglobulin (IVIG) has been used as an important therapeutic drug for many clinical conditions, such as primary immunodeficiency and autoimmune diseases and acute inflammatory conditions, for a long time (8). IVIG acts based on the function of natural antibodies, a factor of homeostasis maintenance in healthy individuals (9). It is also assumed to exhibit an immunomodulatory action against incontinence of the immunoregulatory system